Delft University of Technology

Towards real-time ship collision risk analysis

An improved R-TCR model considering target ship motion uncertainty

Li, Mengxia; Mou, Junmin; Chen, Pengfei; Rong, Hao; Chen, Linying; van Gelder, P. H.A.J.M.

Important note
To cite this publication, please use the final published version (if applicable).
Please check the document version above.

Towards real-time ship collision risk analysis: An improved R-TCR model considering target ship motion uncertainty

Mengxia Li [a,b,c], Junmin Mou [a,b], Pengfei Chen [a,b,*], Hao Rong [d], Linying Chen [a,b], P.H.A.J.M. van Gelder [c]

[a] School of Navigation, Wuhan University of Technology, Wuhan, China
[b] Hubei Key Laboratory of Inland Shipping Technology, Wuhan, China
[c] Safety and Security Science Group, Faculty of Technology, Policy and Management, Delft University of Technology, Delft, the Netherlands
[d] Centre for Marine Technology and Ocean Engineering (CENTEC), Instituto Superior Técnico, Universidade de Lisboa, Av. Rovisco Pais, Lisboa, Portugal

ABSTRACT

Collision between ships is one of the major contributors to ship accidents. To facilitate the development of the real-time collision risk analysis model for collision avoidance, in this research, an improved Rule-aware Time-varying Collision risk Model is proposed, which considers the estimation of target ship motion and the corresponding uncertainty in the risk analysis process. To make the collision risk model more in line with the actual situation, ship maneuverability, the COLREGs, and good seamanship are considered and integrated into the framework of the TCR model. Firstly, the Gaussian process is used to predict the potential trajectories of the target ship. Secondly, the Probabilistic Velocity Obstacle (PVO) model is utilized to integrate the uncertainty of the target ship's motion into the collision risk model. The collision risk is therefore formulated as a ratio of available maneuvers leading to a collision to all available maneuvers. To verify the effectiveness of collision risk, two actual target ships and six groups of collision risk detection experiments under different encounter scenarios were carried out. Compared with the traditional collision risk index model and original R-TCR model, the collision risk detected by the Improved R-TCR model is closer to the actual situation.

1. Introduction

Maritime transportation is one of the major contributors to global economic development [1]. However, accidents such as the collision between ships have been posing practical threats to individuals and societies with dire consequences in terms of loss of life, economic loss, and the environmental pollution, etc. [2,3]. To facilitate the prevention of the collision between ships and to improve the safety level of the maritime transportation system, the significance to identify the collision risk among ships has already been accepted by both the industry and academia [4,5].

To fulfill such an objective, considerable efforts have been devoted by the researchers. Collision risk index (CRI), Safety boundary approach, Binary collision criteria method, Probability of collision method, Dangerous region method Action lines method, etc. have been widely used in collision risk modeling. The detailed literature review is elaborated in Section 2. Among the recent development in the modeling of ship collision risk, the uncertainty of target ship motion is one of the

important factors which is yet not fully considered. This leads to the unreliability of the risk model, which also affects the reliability of collision avoidance decisions.

To further improve the accuracy and avoid misestimation of collision risk, based on the previous work by the authors [6], this paper proposed a Velocity obstacle-based, comprehensive collision risk modeling method that takes target ship motion uncertainty, Convention on the International Regulations for Preventing Collisions at Sea (COLREGs), own ship maneuverability, and good seamanship into consideration, which is the Improved Rule-aware Time-varying Collision Risk model. The Gaussian process is used to predict the target ship trajectory, and the Probabilistic Velocity Obstacle (PVO) algorithm is used to integrate multiple factors into the collision risk model. Considering the objective of the research, the contribution is two-fold: (1) With the consideration of the prediction of future motion characteristics of both the own ship and target ships, the analysis of the encounter situation and the risk of collision can include the motion trend of the ships together with their corresponding uncertainties. (2) With the integration of the collision

avoidance rules and regulations, such as COLREGs, the risk analysis on the ship encounters can provide results that better incorporate the practices of navigation and therefore, have higher values for applications in real situations.

To fully elaborate on the details of the proposed method and the corresponding analysis, the content of the paper is arranged as follows: Section 2 illustrates the methodology of the research and the details of the component of the proposed collision risk analysis model. Section 3 gives the results of the case study, which is to verify the effectiveness of the method, followed by a detailed analysis of the proposed model and a comparison of the performance between the new method and the original TCR models. Section 5 concludes the research.

2. Literature review

Various works have been conducted regarding the modeling of collision risk between ships [7] summarized these methods into three different types of collision risk numerical models: methods based on traffic flow theory, ship domain, and methods based on the distance to the Closest Point of Approach (CPA) and Time to Closest Point of Approach (tCPA). Different classification standards will have different classification results. Two main approaches are proposed to model the collision risk between ships, which are the Expert-based method and the Model-based method, respectively [8]. The Expert-based method relies on experienced experts to evaluate the collision risk of the encounters, and the results reflect the experts' views on the collision event. This method can be divided into two categories: one is the collision risk index (CRI) approach, and the other is the safety boundary approach [8]. CRI is the result of a comprehensive evaluation of risk-related various indicators based on expert knowledge, which represents the risk of the current encounter situation [9,10] comprehensively analyzed the four indexes of relative distance, speed, CPA, and tCPA to calculate the collision risk [11] proposed a judgmental expert-based process to assess the ship collision risk using multiple criteria outranking method. The Margin of Projected Collision (MPC) index is a new risk index, which is the same as CPA index can represent the proximity of ships in space and time and provide collision warning for ships [12]. The Vessel Conflict Ranking Operator (VCRO) method converts the distance between the two ships, the relative speed of the ships, and the difference between the headings of the ships to a risk value [13]. The safety boundary approach is to analyze the collision risk according to the set safety area surrounding the ship. When the ship or obstacle enters or is about to enter the safety area, it is considered that there is a collision risk [14]. On the basis of the degree of domain violation, a new collision risk model based on ship domain [15] is proposed by adding the relative speed of the two vessels, the combination of the vessels' courses, arena violations, encounter complexity, etc. The fuzzy logic method is used to determine the ship domain and calculate the collision risk between ships by judging the relationship between CPA and the fuzzy ship domain [16]. Through the combination of Support Vector Machine (SVM) and ship domain, the margin between ship domains of own ship (OS) and the target ship (TS) used to simulate collision probability is reconsidered, and a quantitative evaluation model of ship collision risk is proposed [17]. In general, these methods are highly reliant on the knowledge of the experts to determine the key parameters in the risk models, and the results are limited by the level of knowledge and experience of experts.

The model-based method analyzes the collision risk by quantifying the collision probability between ships. Most of them quantitatively calculate the possibility of the collision accident on the premise of the assumption that the target ships keep their initial speed and course during the encounter process. This assumption simplifies the physical process of collision. The model-based method can be divided into four categories: (1) the Binary collision criteria method; (2) the Probability of collision method; (3) the Dangerous region method; and (4) the Action lines method. The binary collision criteria method mainly depends on parameters such as CPA and tCPA. If CPA is less than the safe distance

and tCPA is positive, it is considered that there is a collision risk. The probability of collision method uses probability to measure the collision risk during ship navigation. There are many methods for constructing collision risk probability function, such as Monte Carlo simulation [18], probability flow [19], etc. These methods take into account the uncertainty of the collision process to a certain extent. However, most of these methods are limited when estimating the collision risk together with its uncertainty. Due to the lack of historical data, it is difficult to obtain the uncertainty of the encounter process, hence its influence on the collision risk. The dangerous region method can be divided into two categories: one is to find the velocity obstacle set in the velocity space and conduct risk modeling by judging whether the current speed is in the velocity obstacle set [1,6,20]; Another is in the geospatial domain, and risk identification is carried out by judging whether the ship will invade the dangerous region when keeping the current speed and course, such as the predicted area of dangers (PAD) [21], Obstacle Zone by Target (OZT) [22], etc. The last is the action line method, which means that the ship obtains the action line by avoiding collision through ship maneuvering (course change and speed change). The action line can be obtained by operating the ship repeatedly. The collision risk can be calculated by the proportion of the action line of collision avoidance failure [23].

To sum up, the above collision risk models have different forms [4]. However, there is no reliable method to take the uncertainty of target ship motion into account in risk modeling. It is therefore of great significance to integrate the uncertainty of target ship motion into risk modeling to improve the accuracy of the model. At present, various methods are used to solve the uncertainty of target ship motion, which are summarized as the safe distance method and trajectory prediction method. The safe distance method is to increase the safe distance between two ships. The influence of the target ship motion uncertainty on safety can be ignored. There is a deterministic distance method [24,25] and a probabilistic distance method [26] in the existing research. The method of expanding the safety distance to reduce the uncertainty impact of the target ship is usually applicable to open waters. In restricted waters, due to the limitation of water space, the risk modeling could cause false alarms with inappropriate settings of the safety domain. The trajectory prediction method is to predict the future target ship's motion. It can be realized by analyzing the historical trajectory by using the dynamic Bayesian network [27], neural network [28], adaptive filtering algorithm [29], probability obstacle method [30], etc., but these methods are often suitable for short-time motion behavior prediction, and the prediction accuracy of long-time motion behavior is not high [31] combined the method of increasing safety distance and linear prediction model to reduce the interference caused by the uncertainty of target ship motion and established the collision risk modeling between ships. However, ship trajectory prediction itself has certain uncertainty, and its prediction accuracy cannot be guaranteed to a large extent. This is because the ship's movement is affected by Officers On Watch (OOW)'s intention, wind, waves, target ship movements, and other external factors in a complicated manner. Some researchers have contributed their ideas on solving these issues, e.g. [32] relied on the information interaction between ships to obtain the target ship trajectory information [33] predict the ship trajectory based on the route fitting model and Gaussian process. The application of Gaussian process [34] in ship trajectory prediction makes it possible to solve the problem of target ship motion uncertainty in the field of risk.

Analytical approximations method [35], Monte Carlo method [32], Gridding methods [36], Markov chain approximations [37] and Probabilistic Velocity Obstacle (PVO) method [8] can solve the problem of uncertainty in modeling. These methods have their advantages and are rarely used in ship collision risk modeling. The velocity obstacle method is a simple and fast calculation method, which has been widely used in the field of collision risk [4,5,38]. PVO is an improvement based on the velocity obstacle method. It perfectly absorbs the advantages of the velocity obstacle method and can integrate ship maneuverability and other constraints to provide a solution for risk modeling considering

uncertainty.

To overcome the challenges of uncertainty and the complicated encounter situation for the accurate collision risk modeling, in this paper, the PVO algorithm is used to integrate the uncertainty of target motion, ship maneuverability, COLREGs and good seamanship into the collision risk model.

3. Methodology

The objective of this paper is to propose a collision risk model considering the target ship's motion uncertainty with a prediction approach. This paper can be divided into two parts, one is the trajectory prediction model, and the other one is the collision risk modeling.

The trajectory prediction model uses continuous probability distribution to describe the ship motion uncertainty by Gaussian Process [33]. Target ship trajectory prediction is also the ship motion intention estimation. Firstly, historical AIS data need to be clustered to identify the main route, including route boundary and centerline, to build the route model. Then, the parameters used to describe the trajectory characteristics are trained from the historical AIS data, such as longitudinal acceleration probability distribution, hyperparameters of the Gaussian process, etc. Finally, the trajectory prediction is realized by the Gaussian process and projected into the route model to realize the final target ship trajectory prediction. The output of the trajectory prediction model is a
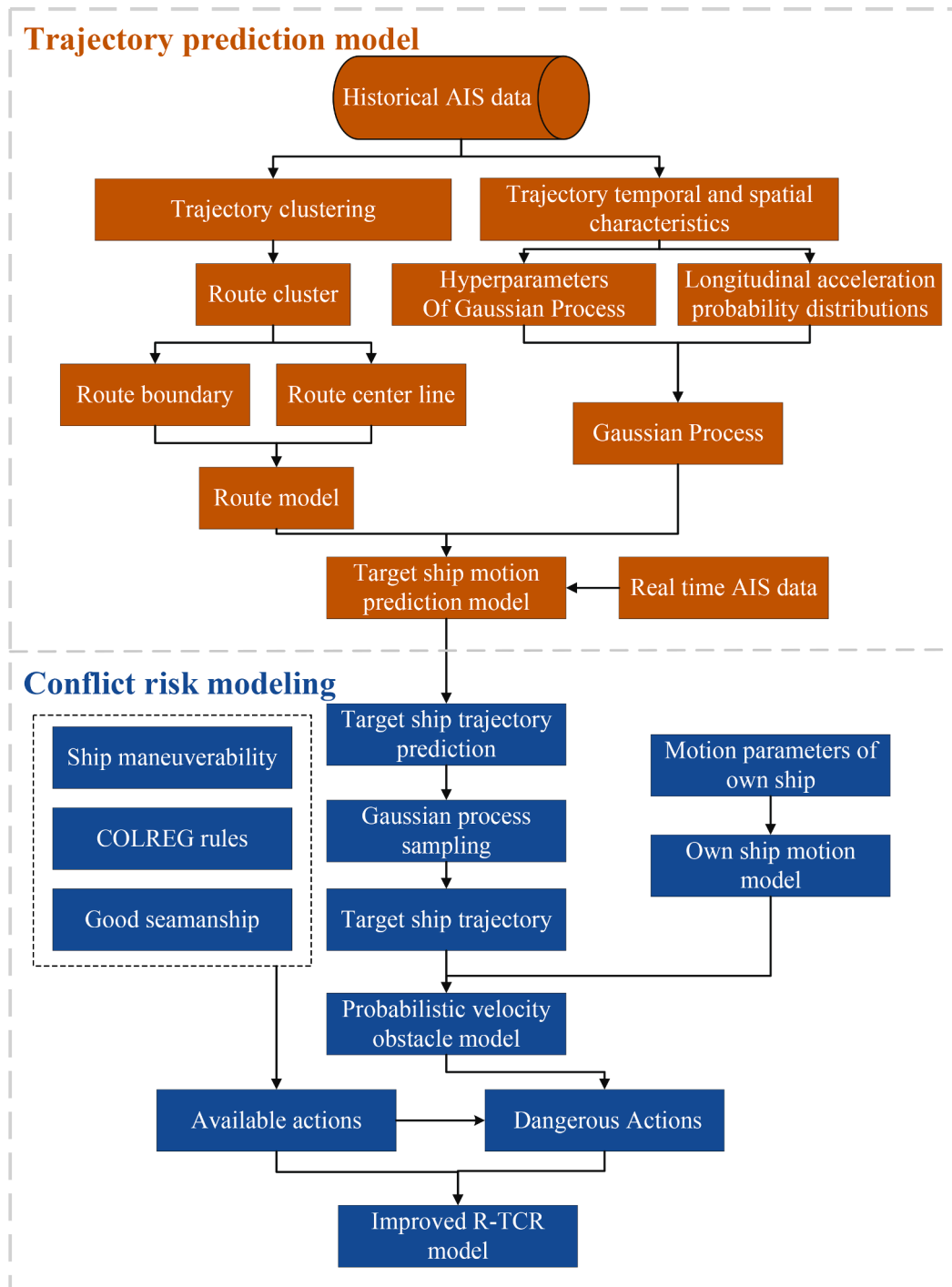

Fig. 1. The framework of the research.

series of possible trajectory points, rather than a single trajectory.

The second part is collision risk modeling. Firstly, the trajectory prediction model proposed in the first part is applied to predict the possible trajectory points of the target ship. Then, according to the three observation points, a certain number of possible ship trajectories are sampled by the posterior Gaussian process. These sampled ship trajectories will be used for the calculation of the collision risk. Then, the PVO method is introduced to determine the potential own ship's actions that will lead to collision by considering COLREG rules, good seamanship, and ship maneuverability. The available actions are identified based on the aforementioned factors. Improved R-TCR is formulated as the percentage of the available action that leads to violation of the ship domain. Finally, the collision risk is calculated by using the Improved R-TCR model to quantify the collision risk between ships. The flowchart of the principal methodology can be found in Fig. 1.

3.1. Trajectory prediction model

This section elaborates on the trajectory prediction model, which is to obtain the predicted trajectory of the target ship considering the uncertainty. The route model, the longitudinal motion part, and the lateral motion distribution of the ship constitute the traffic motion patterns. The detailed designs of the models are discussed in the following sections:

3.1.1. Route identification

The objective of the route identification model is to identify the ship route from the historical ship traffic data and to facilitate the development of the motion prediction model of the target ship. When a ship sails, it often sails along a fixed route. In the water area of the Traffic Separation System (TSS), the ship strictly follows the navigation regulations of the traffic separation system and generally navigates along the route at the center of the specified traffic lane. The route is obvious in the waters of the fixed channel and TSS. However, in the waters without a fixed channel, ships will also sail along a route that normally forms from the experience of the ship officer and does not have specific waterway information. To facilitate the identification of ship routes with a high level of generalization, especially in the areas without specific ship routes, the route identification model is proposed. Such a model could also facilitate the establishment of the TSS system in the areas where there is complicated ship traffic but no specific ship routes.

Through the historical trajectory data, the ship trajectories can be classified into various clusters according to their characteristics. The trajectories with the same characteristics are divided into a group, and the trajectories of the same group together form a usual and customary route. The most common route identification method is clustering. In this paper, the Density-Based Spatial Clustering of Applications with Noise (DBSCAN) algorithm will be used for trajectory clustering [39] firstly proposed DBSCAN in 1996. It is a density-based clustering non-parametric algorithm. Given a set of points in some space, it groups together points that are closely packed together (points with many nearby neighbors) and identifies the outliers that lie alone in low-density regions (whose nearest neighbors are too far away).

DBSCAN requires two parameters: ε and minPts. ε is a parameter specifying the radius of a neighborhood with respect to some point. minPts is the minimum number of points required to form a dense region within the ε radius. It starts with an arbitrary starting point that has not been visited. This point's ε-neighborhood is retrieved, and if it contains sufficiently many points, a cluster is started. Otherwise, the point is labeled as noise.

As shown in Fig. 2, the radius of each large circle in the figure is ε, minPts = 4. The red points are core points because the area surrounding these points in an ε radius contain at least 4 points (including the point itself). Because they are all reachable from one another, they form a single cluster. Green points are not core points, but are reachable from A (via other core points) and thus belong to the cluster as well. A blue
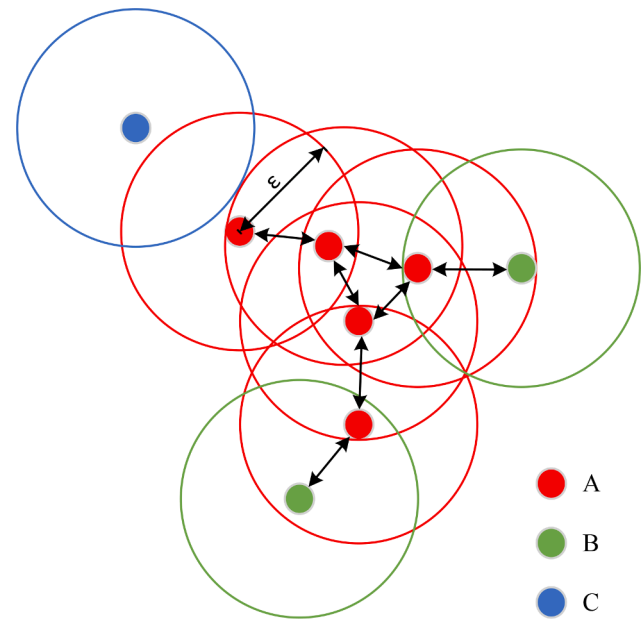

Fig. 2. DBSCAN clustering diagram.

point is a noise point that is neither a core point nor density-reachable. When DBSCAN is applied to ship trajectory clustering, the distance between trajectories needs to be considered.

The route identification model can be composed of route characteristics such as route boundary and centerline. After trajectory clustering, the trajectory in the water area will be divided into several clusters. Each cluster is a trajectory band. The boundary and centerline of each trajectory cluster need to be extracted. The route boundary refers to the outer boundary that can include a group of trajectory clusters, and the route centerline refers to the centerline of the outer boundary of the route, as shown in Fig. 3. The boundary and centerline of the route can be represented by key points.

3.1.2. Motion prediction model

The premise of trajectory prediction is to assume that the ship navigates along the route or usual and customary route, and does not change its set route during navigation. The set route is generally parallel to the centerline of the route. The ship motion is decomposed into the motion along the set route and the motion perpendicular to the set route, that is, longitudinal motion and lateral motion.

To better describe the ship's longitudinal and lateral motion, the route-fitted coordinate system is adopted in this paper [33]. The coordinate system takes the route centerline as the reference and transforms the longitude and latitude coordinates into equivalent coordinates in the routing space, as shown in Fig. 4.

According to the above description, the ship's position can be decomposed into longitudinal and lateral. The ship's longitudinal and lateral position distributions can be obtained by integrating the ship's longitudinal and lateral accelerations, respectively. The probability density of longitudinal acceleration is determined by statistical analysis of historical AIS data of the research water area. The probability density of lateral acceleration is estimated by the Gaussian process model. The hyperparameters of the Gaussian process are obtained from historical AIS data.

(1) Longitudinal motion model

Longitudinal motion means that the ship moves along the centerline parallel to the route or usual and customary route. However, the ship's speed and acceleration when it reaches each position are not consistent. Therefore, to describe the longitudinal uncertainty of the ship, the
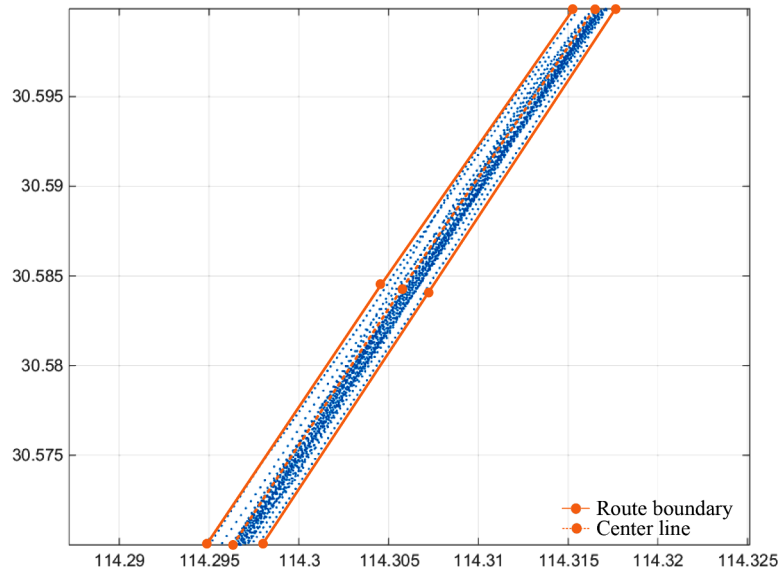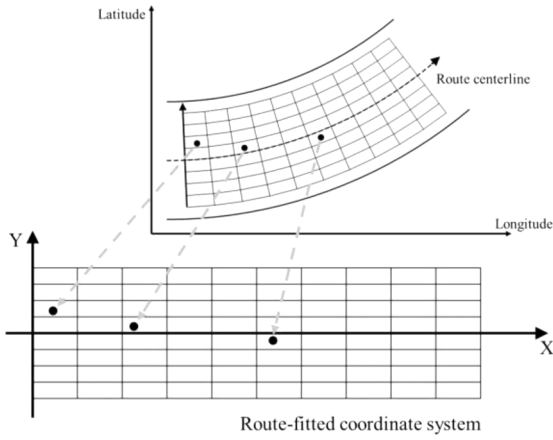
Fig. 3. Route diagram.

Fig. 4. Route-fitted coordinate system [57].

acceleration of each position point is obtained from the historical AIS data. To describe the acceleration of each position conveniently, the acceleration probability distribution model is simplified, as shown in Eq. (1). In this paper, the longitudinal spacing when extracting the longitudinal acceleration is 1000m.

$$a_{px} = f(px) \tag{1}$$

Where: px refers to the longitudinal position of the ship, a_{px} represents the acceleration of the ship's longitudinal position (px).

Ship longitudinal position of the ship can be calculated by Eq. (2):

$$x_* = x_0 + v_0 t + \frac{1}{2} a_{px} t^2 \tag{2}$$

Where: x_* represents the predicted longitudinal position of the ship; v_0 represents ship initial speed; t represents sailing time.

(2) Lateral motion model

The Gaussian process is a stochastic process specified by its mean and covariance function [40]. Every finite set of random variables in the Gaussian process has a multivariate normal distribution, that is, every finite linear combination is a normal distribution. The distribution of the Gaussian process is the joint distribution of all these (infinite) random variables. Therefore, it is the distribution of a function with a continuous domain (such as time or space). In this study, the Gaussian process is used to predict the lateral position of the ship along the ship's route. Gaussian process describes the lateral uncertainty of ship trajectory through a set of mean and covariance functions, and conditionally predicts the lateral position of the ship through new observation data and previous observation values, as shown in Eq. (3).

$$f(x) \sim \mathscr{GP}(m(x), k(x, x')) \tag{3}$$

where $m(x)$ is the function used to calculate the mean; $k(x, x')$ is the covariance function, which is used to describe the information coupling between independent variables x and x'.

A major advantage of using the Gaussian Process is that functions can be conveniently specified by a mean function $m(x)$ and a covariance function $k(x, x')$, as:

$$m(x) = \mathbb{E}[f(x)] \tag{4}$$

$$k(x, x') = \mathbb{E}[(f(x) - m(x))(f(x') - m(x'))] \tag{5}$$

where $\mathbb{E}[\cdot]$ denotes the expectation operator and $k(x, x')$ is a covariance function that describes the information coupling between independent variable x and x'.

In this study, the most commonly used squared exponential covariance function is adopted, the formula is as follows:

$$k(x_p, x_q) = \sigma_f exp\left(-\frac{\| x_p - x_q \|}{2l}\right) \tag{6}$$

where: σ_f and l are hyperparameters; σ_f denotes the amplitude that specifies the maximum allowable covariance. l is the length scale parameter, which defines the rate of decay in correlation for points further away from each other; $\| \cdot \|$ is Euclidean distance between two vectors.

The covariance matrix in the Gaussian process is the Gram matrix, and the formula is as follows:

$$K(X, X) = \begin{bmatrix} k(x_1, x_1) & k(x_1, x_2) & k(x_1, x_N) \\ & \cdots & \\ k(x_2, x_1) & k(x_2, x_2) & k(x_2, x_N) \\ \vdots & \ddots & \vdots \\ k(x_N, x_1) & k(x_N, x_2) & \cdots k(x_N, x_N) \end{bmatrix} + \sigma_{noise}^2 I_N \tag{7}$$

where: I_N is the identity matrix of size N.

The joint distribution of observed and predicted values at the sample location can be expressed as:

$$\begin{bmatrix} Y \\ Y_* \end{bmatrix} \sim \mathcal{N}\left(0, \begin{bmatrix} K(X,X)_{N \times N} & K(X,X_*)_{N \times N_*} \\ K(X_*,X)_{N_* \times N} & K(X_*,X_*)_{N_* \times N_*} \end{bmatrix}\right) \quad (8)$$

where: $X = (x_1, \ldots, x_N)^T$ represents the observations, $X_* = (x_{*1}, \ldots, x_{*N_*})$ is the vector of N_* values for which the lateral position $Y_* = (y_{*1}, \ldots, y_{*N_*})$ are predicted.

The nature of the Gaussian Process is such that, conditional on observed data, predictions can be made about the function values, $f(x_*)$ at any location x_*. The distribution of these values at x_* is Gaussian with mean and covariance, given as:

$$\mu(x_*) = m(x) + k(x_*,x)K^{-1}(y - m(x)) \quad (9)$$

$$\sigma^2(x_*) = K(x_*,x_*) - K(x_*,x)K^{-1}K(x_*,x)^{\top} \quad (10)$$

As shown in Fig. 5(a), the Gaussian Process model provides the underlying trajectory with a 95% confidence interval. Grey circles represent observations, the red line represents the predicted mean trajectory, and the red region represents the predicted 95% confidence bounds. It can be seen that the predictive uncertainty grows if the ship was not observed for a long time, and the prediction bounds are wide and open to the right until a new observation is included in the Gaussian Process prediction model. Fig. 5(b) shows some sampled ship trajectories from the posterior Gaussian Process. The sampled ship trajectories will be used for the collision risk model.

3.2. Collision risk model

In this section, we propose an Improved Rule-aware Time-varying Collision Risk (Improved R-TCR) measurement model for ship collision risk detection. The model further considers the uncertainty of target ship motion based on considering the maneuverability of the OS, COLREG rules, and good seamanship. The definition and methods of the risk model will be proposed here.

3.2.1. Definitions

There are many forms of risk, and the research on collision risk mainly focuses on collision probability. In addition, there are some new collision risk concepts, which integrate the percentage of maneuvers in which the ship cannot avoid the collision(Time-varying Collison Risk, TCR) [41]. Based on TCR [6], combined maneuverability of the OS, COLREG rules, and good seamanship to propose a definition of Rule-aware Time-varying Conflict Risk (R-TCR). This paper accepts the risk definition of TCR. Collision in this paper refers to the event that a TS violates the OS's domain.

Definition 1. Improved Rule-aware Time-varying Collision risk is the probability of the violation of the OS's ship domain by target ships in this paper.

Definition 2. Available action (AA) is a set of course and speed that OS can reach at the current juncture, considering COLREGs.

Definition 3. Dangerous action (DA) is a subset of AA that includes courses and speed of the OS that could lead to a collision between the OS and the TSs.

Based on the aforementioned, the calculation process of R-TCR is as follows.

$$R - TCR = \frac{n(DA)}{n(AA)} \quad (11)$$

Where: $n(DA)$ is the number of dangerous actions of OS; $n(AA)$ is the number of available actions of OS.

Since the Improved R-TCR model takes into account the target ship's motion uncertainty, there are countless possibilities for the target ship's trajectory after the Gaussian process is used to predict the target ship's motion. The calculation diagram of dangerous action set under different encounter situations is shown in Fig. 6. k trajectories are extracted by the posterior Gaussian sampling for risk calculation, as shown in Fig. 6 (a). In this paper, the target ship trajectory is decomposed. Each possible target ship trajectory corresponds to OS one by one, and the dangerous action of the ship for any target ship trajectory is calculated. Combined with the probability of each target ship's trajectory, the probabilistic dangerous action set of two ships' encounter situations can be calculated, as shown in Fig. 6 (b). Fig. 6 (c) represents a schematic diagram of a multi-ship encounter situation, in which each target ship uses posterior Gaussian sampling to extract k target ship trajectories. Similarly, any trajectory of each target ship forms a multi-ship encounter situation with OS, and the dangerous action set of each possible multi-ship encounter situation is calculated. Combined with the probability of each situation, the probability dangerous action set of the multi-ship encounter situation can be calculated, as shown in Fig. 6 (d).

The equation of the Improved R-TCR is as follows:

$$\text{Improved} R - TCR = \sum_{j=1}^{k^s} P_{(j)} \times \frac{n(DA_j)}{n(AA_j)} \quad (12)$$
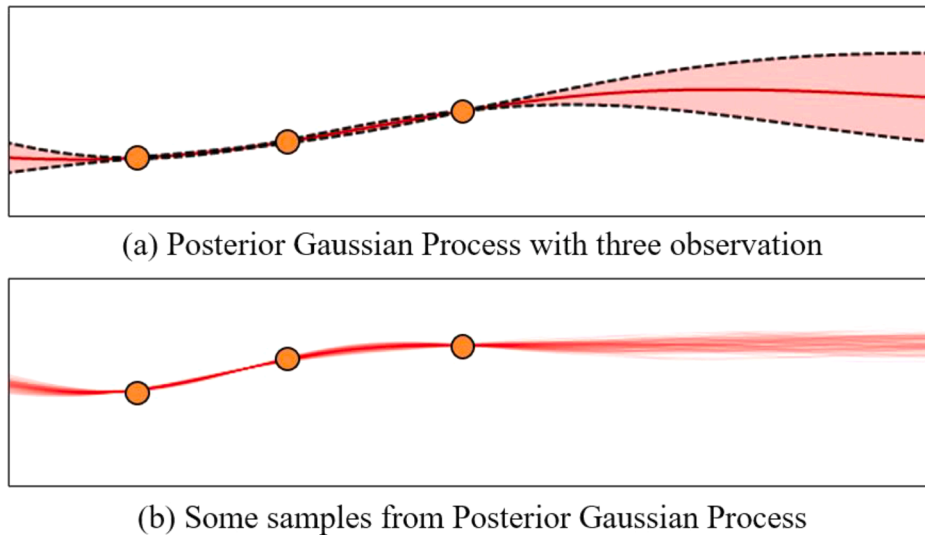

(a) Posterior Gaussian Process with three observation

(b) Some samples from Posterior Gaussian Process

Fig. 5. Illustration of trajectory sampling from Gaussian process [33].
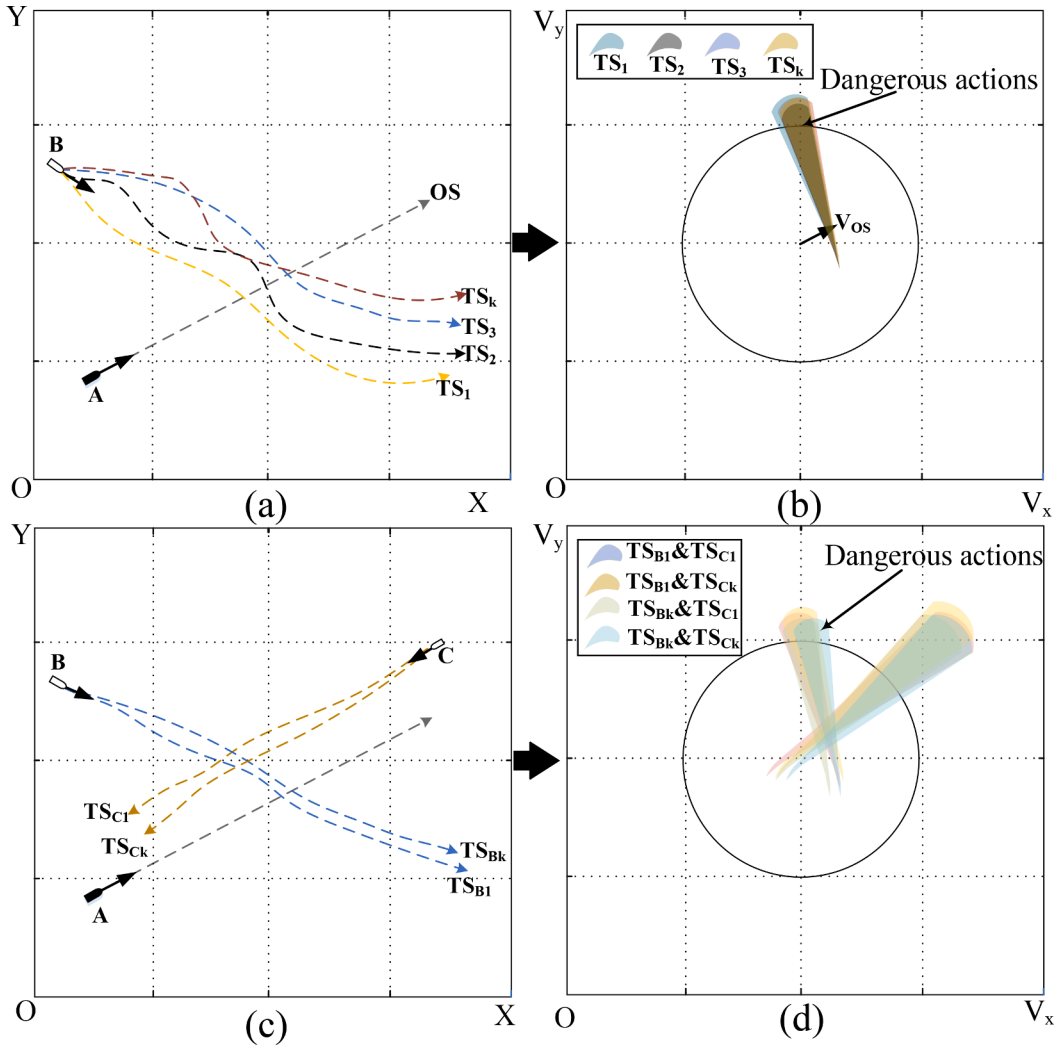
Fig. 6. Encounter situation under TS motion uncertainty.

$$\sum_{j=1}^{k^s} \mathrm{P}_{(j)} = 1 \qquad (13)$$

where: $\mathrm{P}_{(j)}$ is the probability of the jth possible encounter situation; $n(DA_j)$ is the number of dangerous actions in the jth possible encounter situation; $n(AA_j)$ is the number of available actions in the jth possible encounter situation; k represents the number of trajectories sampled by one target ship; s represents the number of target ships.

3.2.2. Available actions

Improved R-TCR refers to the ratio of dangerous action set to available action set, which represents the possibility of the ship avoiding the collision accident. Available action is a set of courses and speed that OS can reach at the current juncture, considering COLREGs and good seamanship.

When there is a collision risk between two ships, the give-way ship needs to take certain avoidance actions to avoid the collision. According to rule 8 of the COLREGs, course alteration is the most effective action to avoid collision under most circumstances, especially at the open sea when ample sea room is available. Speed alteration is also a kind of avoidance measure only when there is a close-quarter situation. The experience of the crew is very important in the choice of collision avoidance action [42]. According to the OOWs' preferences and the limitations of the rudder, the range of course changes usually would not be larger than 90 deg [43,44]. Moreover, different encounter situations

might lead to different rule-aware available course range. The rule-aware available course ranges for head-on, crossing, and overtaking situation are [0°, 90°], [0°, 90°] and [-90°, 90°], respectively [43,44]. A positive value represents an altered course to the starboard, and a negative value represents an altered course to the port side. when the ship needs to alter course to avoid the collision, all possible courses C are discretized at regular intervals (1°). When the ship needs to slow down to avoid the collision, it generally does not adopt astern order. The engine order can be expressed as E=[Ahead NAVI. Full, Ahead Full, Ahead Half, Ahead Slow, Ahead Dead Slow, Stop].

Engine order and course order are paired one by one. At each time, there is an available action set composed of several engine orders and course orders.

When E_0 is not Ahead NAVI. Full, E can be any value less than or equal to E_0. The available actions are shown in Eq. (14).

$$f(t, C, E) = \begin{bmatrix} (C_{t1}, E_{t1}), \dots, (C_{t1}, E_{tn}) \\ \dots\dots \\ (C_{tm}, E_{t1}), \dots, (C_{tm}, E_{tn}) \end{bmatrix} \qquad (14)$$

Where: t represents time; E represents engine order; C represents course alteration; n represents the number of available engine orders, and m represents the number of available course orders.

However, when the ship is in Ahead NAVI. Full order, to protect the main engine, it generally only adopts alter course to avoid the collision. The engine order in all action sets is E_0 and remains unchanged. The

available actions under this situation are shown in Eq. (15). This means that in this mode, only course alteration is selected to avoid the collision.

$$f(t, C, E) = \begin{bmatrix} (C_{t1}, E_0) \\ ...... \\ (C_{tm}, E_0) \end{bmatrix} \qquad (15)$$

3.2.3. Dangerous actions

The calculation method of available action sets has been calculated in Section 3.2.2. Hence, to calculate Improved R-TCR, it is also necessary to solve the number of dangerous action sets. Dangerous Action (DA) is a subset of AA that includes courses and speed of the OS that could lead to the collision between the OS and the TSs. To find out the dangerous action in available action, the enumeration method will be used to calculate each action. As shown in Fig. 7, When there are k target ship trajectories, they can be decomposed into k pairwise combinations of the TS and OS. When OS selects avoidance actions from the available avoidance action set, OS will start navigating according to the ship motion model. The distance between ships is constantly changing. $D^{(1)}$ and $D^{(2)}$ in the figure represent the distance between two ships at different times. When the TSs enter the OS's domain, the avoidance action selected by OS at this time is a dangerous action.

(1) Ship domains

The ship domain refers to an area surrounding the ship where other ships are not welcome to enter [45]. The ship domain has been widely used in collision risk modeling [46]. Therefore, it is very important to determine a practical ship domain for risk modeling. According to the ship domain modeling method, it can be divided into Empirical (statistical), and knowledge-based approaches [47].

The empirical domain is obtained through statistical analysis of historical data including radar, AIS, and maritime surveys [45] originally proposed the elliptical ship domain with the OS ship in the center through observation radar data [48] observed the influence of COLREGs and developed a new ship domain with an integration of 3 different sectors [49] smoothed the integrations with a circle boundary and set a "phantom ship" in the center for easy expression in math. Through AIS data, the ship domain is established, such as ship domain based on risk perception [50], ship domain for traffic separation system waters [51] and probabilistic ship domain [52].

The knowledge-based method is to integrate the crew's knowledge and experience into the modeling through the intelligent algorithm [47] and [53] use fuzzy method to integrate experience and establish the ship domain. The method based on empirical analysis has certain objective properties, but it lacks empirical correction. The method based on knowledge has certain subjectivity. Therefore, the combination of the two methods is helpful to make the ship domain model more practical. Some studies have conducted a preliminary study here [54].

Based on the statistical method and expert experience, this paper adopts a dynamic ship domain according to different encounter situations, which is illustrated in [6], as shown in Fig. 8. According to COLREGs, the TSs in different encounter situations are located in different directions, and the threat degree to different directions of OS is different. For example, in a head-on encounter situation, the two ships approach from the bow, the space ahead of the ship domain is larger than that in the ship's stern, and the elliptical ship domain is selected. Similarly, the overtaking encounter situation is also in the elliptical ship domain. In the crossing encounter situation, the target ships mainly approach the own ship from the OS's port side and starboard side, thus the bow and stern direction of the domain is not larger than the starboard and port side, so the circular ship domain is selected. The ship domain combines the advantages of the Goodwin and Davis model and is a center offset eccentric ship domain. The Phantom Ship is located at the center of the ship domain, not the real ship. The real ship is fixed by a distance and an angle from the phantom ship. The size of the ship domain is not fixed, and the crew can adjust it according to the actual situation.

(2) The relative distance between ships considering ship domains and ship maneuverability

Fig. 9 shows the trajectory of the OS alters its courses and the prediction trajectory of the TS. The phantom ship is to provide convenience for judging whether the domain is infringed by target ships. The distance *Dis* from the TS to the OS's domain boundary can be expressed by Eq. (16).

$$Dis^{(t)} = D^{(t)} - R_T^{(t)} \qquad (16)$$

Where $D^{(t)}$ the distance between the center of the OS's domain and TS at t time; $Dis^{(t)}$ is the distance between TS and the OS's domain boundary
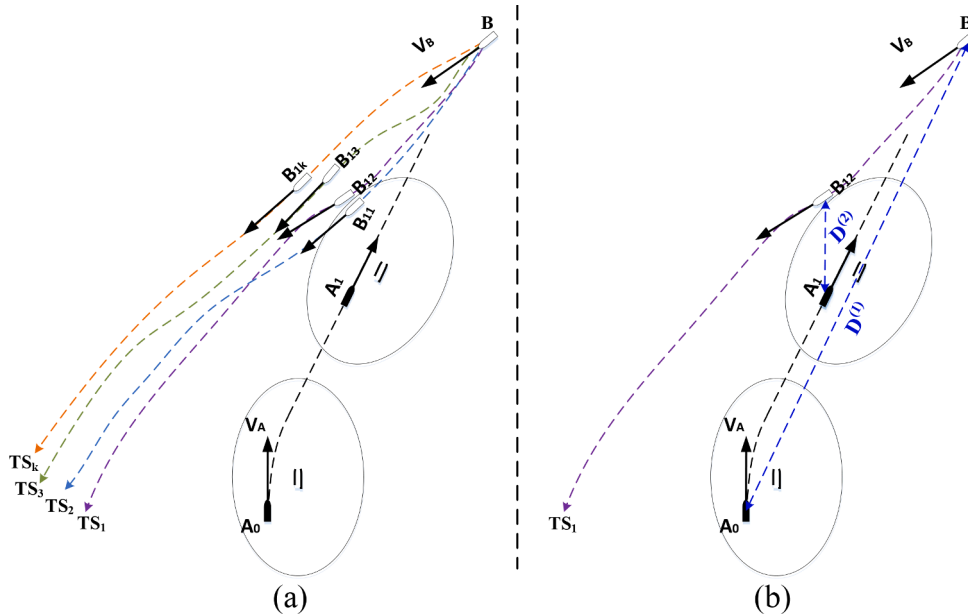

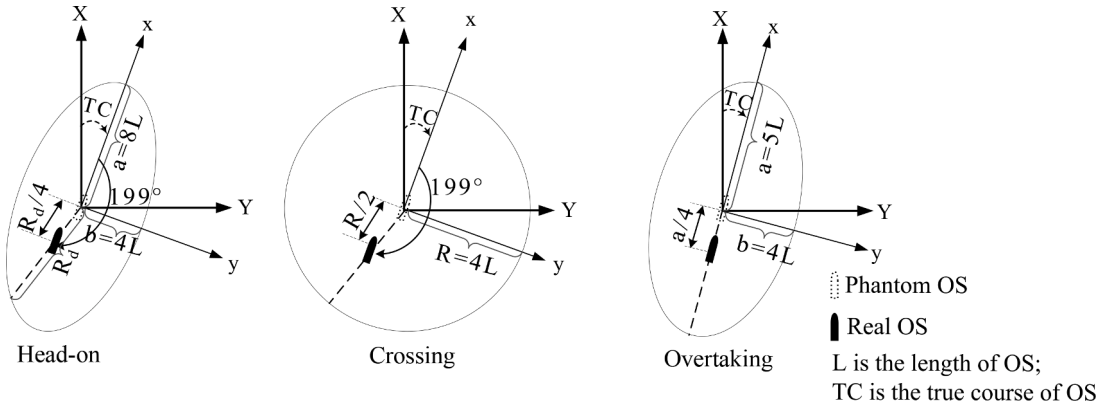**Fig. 7.** OS collision avoidance schematic diagram.

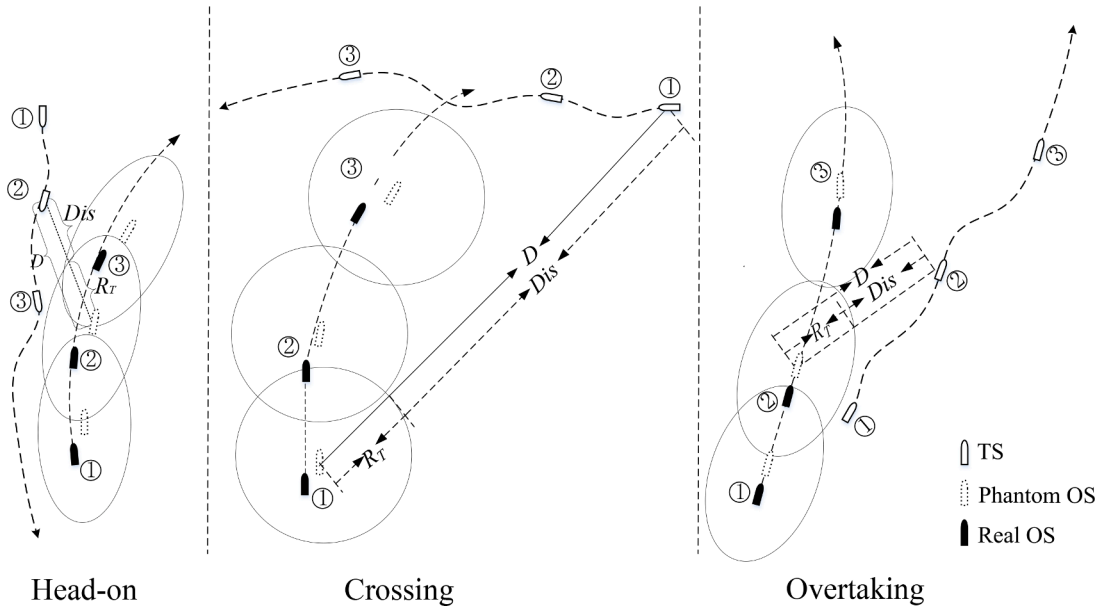**Fig. 8.** Demonstration of the coordinate system and ship domain.

Fig. 9. Process of the OS altering course to avoid collisions.

at t time; $R_T^{(t)}$ is the distance between the phantom ship and the boundary of the OS's domain at t time.

$$D^{(t)} = \sqrt{\left(X_T^{(t)} - X_O^{(t)}\right)^2 + \left(Y_T^{(t)} - Y_O^{(t)}\right)^2} \tag{17}$$

Where:$(X_T^{(t)}, Y_T^{(t)}),(X_O^{(t)}, Y_O^{(t)})$ are the location of TS and OS at time t, respectively. The calculation formula of $R_T^{(t)}$ can be referred to [6].

In order to predict and simulate the maneuvering of OS, three degrees of freedom of ship motion (surge, sway, and yaw) are modeled based on MMG, $(X_O^{(t)}, Y_O^{(t)})$ can be calculated by Eq. (18). Engine order and course are the inputs of the MMG model, and the $(X_O^{(t)}, Y_O^{(t)})$is the output.

$$\begin{cases} (m+m_x)\dot{u} - (m+m_y)vr = X_H + X_P + X_R \\ (m+m_y)\dot{u} - (m+m_x)ur = Y_H + Y_P + Y_R \\ (I_{ZZ} + J_{ZZ})r = N_H + N_P + N_R \end{cases} \tag{18}$$

Where: $m, m_x, m_y, I_{ZZ}, J_{ZZ}$ are mass of the ship, added mass in x and y directions, inertia moment, and additional inertia moment, respectively; Subscript H, P, R are bare hull, propeller, rudder, respectively; u, v, and r denote surge, sway velocity and yaw rate, respectively; X, Y, N are the external forces and moments in different directions, respectively.

The autopilot system is more and more popular in modern ships.

When the course is set, the autopilot system can automatically control the rudder command to achieve the set course. To simulate the process of ship motion control, the fuzzy adaptive Proportion Integral Derivative (PID) control model is used. The fuzzy adaptive PID control principle is shown in Fig. 10. The fuzzy rules used in this paper are from [44,55].

E is the heading error, EC is the error rate of change, and E and EC serve as the inputs of the fuzzy controller. The PID parameters K_P, K_i, K_d serve as the fuzzy controller output. These parameters were adjusted automatically in real-time using the fuzzy control rules based on different E and EC values, i.e., different E and EC pairs are self-tuned for the PID parameters so that the controlled object exhibits good dynamic and static performance.

The trajectory of the target ship can be predicted by the Gaussian process. When the target ship completes the trajectory prediction, a trajectory point set based on time series will be formed, as shown in Eq. (19).

$$\left\{ \left(X_T^t, Y_T^t\right) | \left(X_T^0, Y_T^0\right), \left(X_T^1, Y_T^1\right), ..., \left(X_T^n, Y_T^n\right) \right\} \tag{19}$$

$Dis^{(t)}$ has the following characteristics:
If $Dis^{(t)} > 0$, TS will not enter OS's domain;
If $Dis^{(t)} < 0$, TS will enter the OS's domain;
If $Dis^{(t)} = 0$, TS is tangent to OS's domain.
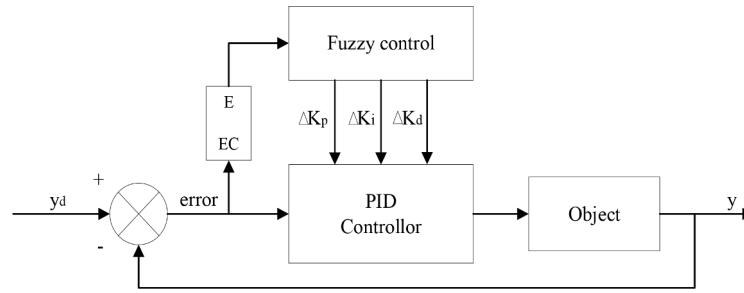According to the value of $Dis^{(t)}$ at different times, it can be deter-

Fig. 10. The principle of fuzzy adaptive PID control.

mined whether the input available avoidance action is dangerous. When the $Dis^{(t)}$ is less than 0, the avoidance action of the OS will be recorded to the dangerous action set; When $Dis^{(t)}$ is always greater than 0, the OS avoidance action is the safety action set. Accordingly, dangerous actions can be calculated with Algorithm 1.

Algorithm 1. Calculation of dangerous actions

Step1. Initial condition setting: MMG model parameter setting, fuzzy PID control model parameter, initial heading, speed, position, and other data of OS, target ship trajectory, and ship domain.

Step2. Set the initial values required for some algorithm loops, such as computing time $t = 0$, initial alter course $C = 0$, initial engine order E_0.

Step3. Based on E_0 and an encounter situation, determine the available actions, and serial numbering all available actions. And count the number of available actions and record it as N, number available action as r.

Step4. If $r \leq N$, input available action corresponding to r into the MMG model, calculate the position of OS at time t, go to the next step; otherwise, end the algorithm.

Step5. Calculate $Dis^{(t)}$ according to the position of OS ship and TS at time t.

Step6. If $Dis^{(t)} < 0$, record the E, C and to dangerous action, r=r+1, go to step 4 set; otherwise, go to the next step.

Step7. End the algorithm

3.2.4. Calculation of improved R-TCR model

According to each possible target ship trajectory and the initial information of OS, the number of available actions, dangerous actions and the probability of each possible target ship trajectory can be solved. Combined with the definition in Section 3.1, according to Eq. (12) for Improved R-TCR, the collision risk considering the uncertainty of target ship motion can be obtained.

4. Case study

To verify the effectiveness of the proposed collision risk modeling method, a case study that considers various encounter situations using real AIS data is presented in this section. Ningbo-Zhoushan in eastern China is the world's third-busiest cargo port. The study area is located in Ningbo, Zhejiang Province. The traffic in this water area is dense, and there are many intersections between ship routes.

AIS data will be used to model the ship collision risk in the water area. AIS data can be provided by the traffic flow Laboratory of Wuhan University of technology. Due to a large amount of AIS data, one day of
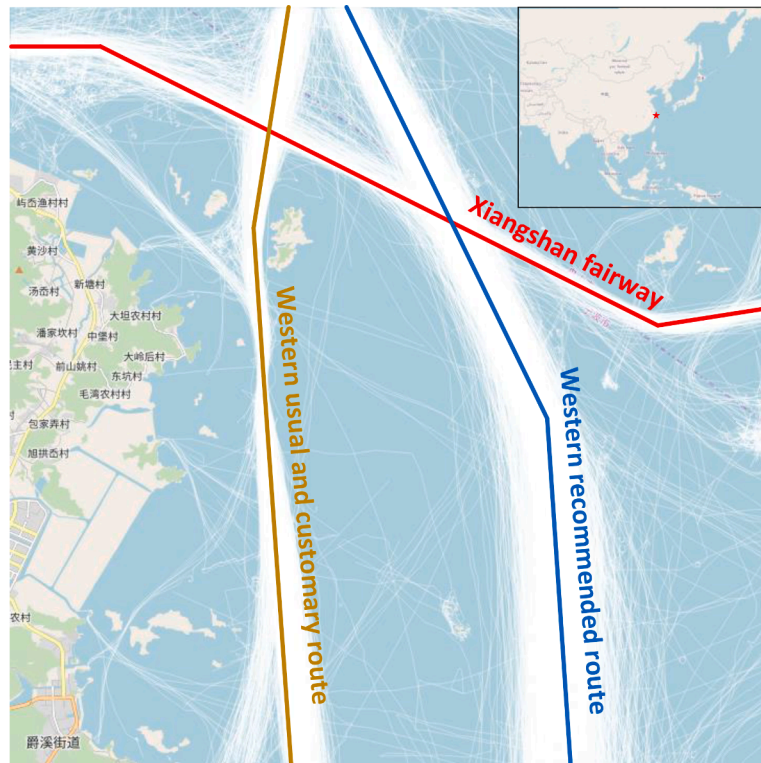

Fig. 11. Illustration of the research area.

AIS data is randomly selected every month from January to July 2019. The ship trajectory diagram is shown in Fig. 11. There are three main routes in the study water area, namely, Xiangshan fairway, Western usual and customary route, and Western recommended route. Western usual and customary route and Western recommended route are North-South routes. Xiangshan fairway is the East-West route. There are two route intersections in the three routes.

4.1. Case setting-up

This paper sets up six groups of classic two ships encounter situations (head-on, crossing, and overtaking) and two groups of multi-ship encounter simulation experiments to verify the reliability and effectiveness of the proposed model.

(1) Setting of OS

In the simulation experiments, a 3DOF MMG model of a Panamax bulk carrier, MV HUAYANG DREAM, is used. Besides, the own ship is set as an unmanned ship, the course changing is controlled by the PID control model. And other ships are manned ships. The related parameters of OS are shown in Table 1.

(2) Setting of TS and OS for two-ship encounter situation

According to different initial states of the target ships and own ships, this paper sets head-on, crossing, and overtaking encounter situations, as shown in Table 2. The layout of the two ship encounter situation is shown in Fig. 12. The Blue ship is TS and the red ship is OS. The CPA of all groups is 0, the tCPA of Group A_1, A_2, B_1, and B_2 are 900s, while the tCPA of Group A_3 and B_3 was 1200 s.

The initial observation values of TSs in the two-ship encounter situations are shown in Table 3. The trajectory observation values of these target ships will be used in the trajectory prediction model to realize trajectory prediction.

(3) Setting of TS and OS when multi-ship encounter simulation

The multi-ship encounter situation is divided into two groups: Group A and Group B. There are two target ships in Group A and three target ships in Group B. The initial state of the ships is shown in Table 4. The layout of the multi-ship encounter situations is shown in Fig. 13.

The observed values of the target ships in multi-ship encounter situations are shown in Table 5.

4.2. Results of trajectory prediction

According to the method described in Section 3.1, the seven days of AIS data are extracted for route model construction and Gaussian process parameter extraction. Combining the route model and Gaussian process parameters, a trajectory prediction model based on the Gaussian process is established. We can use the observed trajectory points of real-time AIS data as input, and the basic trajectory with a 95% confidence interval can be predicted by the Gaussian process trajectory prediction

Table 1
Parameters of OS in simulation.

Parameter	Value	Parameter	Value
Name	HUAYANG DREAM	Displacement (kg)	$90,000 \times 10^3$
Draft (m)	14.5	Breadth (m)	32.5
LOA (m)	225	Density of water (kg/m³)	1025
Block coefficient	0.8715	RPM (r/min)	90
Area of rudder (m²)	56.88	Propeller advance (m)	4.738

Table 2
Initial state of two-ship encounter situations.

	Ship	Longitude/°	Latitude/°	Speed/kn	Course/°	Encounter situation
Group A_1	TS_1	122.0513	29.6339	10.0	122.3	Head-on
	OS_1	122.1483	29.5805	14.0	302.3	
Group A_2	TS_3	122.0439	29.6375	9.80	122.6	Crossing
	OS_3	122.0522	29.6625	13.0	150.0	
Group A_3	TS_5	122.0686	29.6255	9.20	123.4	Overtaking
	OS_5	122.0430	29.6402	14.0	123.4	
Group B_1	TS_2	122.0501	29.6343	13.7	113.9	Head-on
	OS_2	122.1363	29.6011	6.0	293.9	
Group B_2	TS_4	122.0431	29.6371	11.1	114.9	Crossing
	OS_4	122.0626	29.6609	12.0	150.0	
Group B_3	TS_6	122.0681	29.6260	12.8	119.8	Overtaking
	OS_6	122.0526	29.6337	15.6	119.8	

model.

Five clusters are clustered according to the DBSCAN algorithm in Section 3.1.1, as shown in Fig. 14. Trajectory cluster #1, trajectory cluster #2, and trajectory cluster #5 represent Xiangshan fairway, Western usual and custom route, and Western recommended route, respectively. Trajectory cluster #3 and trajectory cluster #4 are two newly discovered clusters from AIS data.

Each trajectory cluster in Fig. 14 is a route. According to the clustered trajectory clusters, the route boundary and centerline are identified, which is shown in Fig. 15.

(1) TSs in two-ship encounter situations

The trajectory observation points will be used as inputs in the proposed trajectory prediction model. The possible trajectory prediction results are shown in Fig. 16. The initial positions of the two ships are very similar, but due to different headings and speeds, the predicted trajectory results are also different.

To further analyze the accuracy of trajectory prediction, we compare the actual AIS trajectory with the predicted trajectory. The trajectories of the two ships are within the range of the predicted trajectories, and the predicted trajectories are consistent with the actual trajectories. This also verifies that the proposed trajectory prediction model can meet the needs of the target ship trajectory prediction for the collision risk model.

(2) TSs in multi-ship encounter situations

Input the observed values of target ships into the prediction model, and the possible trajectory prediction results of TS_{11}, TS_{22}, and TS_{33} are shown in Fig. 17. Similarly, the real trajectories of the three target ships are distributed within the range of predicted trajectories, and the accuracy of predicted trajectories meets the requirements of the collision risk model.

4.3. Results of collision risk analysis

4.3.1. Results of two-ship encounter situations

According to the methods in Section 3.2, for each encounter situation,10 possible trajectories of the target ships will be randomly selected by the posterior Gaussian sampling method. The probabilistic dangerous actions can be calculated by using the PVO method, and the corresponding Improved R-TCR value for each encounter can be obtained according to Eq. (12). The results of collision risk analysis by the Improved R-TCR model, schematic diagram of the encounter situation, and the relative distance between the two ships of the corresponding encounter situations are shown in Figs. 18 and 19. The first columns of each figure are the risk value of the encounter group which is obtained with the Improved R-TCR model. The second column is the real ship trajectory of each encounter situation, and the third column is the relative distances between the two ships that participate in the
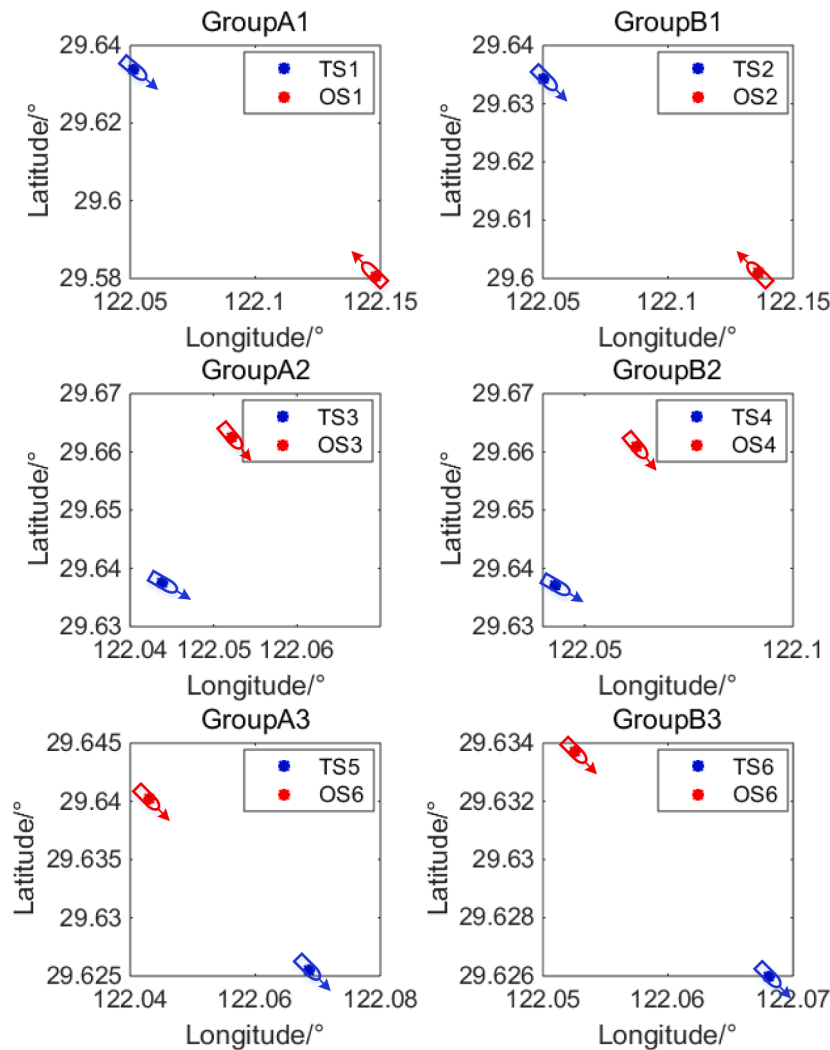
Fig. 12. The planar layout of two-ship encounter situations.

Table 3
Observation values of the target ships in the two-ship encounter situations.

MMSI	Time	Longitude/°	Latitude/°	Speed/kn	Course/°
	2019/1/3 10:21	122.0417	29.6389	9.8	129.1
TS_1	2019/1/3 10:22	122.0439	29.6375	9.8	122.6
	2019/1/3 10:25	122.0513	29.6339	10.0	122.3
TS_2	2019/2/3 12:46	122.0212	29.6456	11.6	115.9
	2019/2/3 12:48	122.0282	29.6427	12.6	115.4
	2019/2/3 12:54	122.0501	29.6343	13.7	113.9
TS_3	2019/1/3 10:19	122.0375	29.6421	9.7	125.8
	2019/1/3 10:21	122.0417	29.6389	9.8	129.1
	2019/1/3 10:22	122.0439	29.6375	9.8	122.6
TS_4	2019/4/3 9:38	121.9894	29.6604	11.1	118.5
	2019/4/3 9:45	122.0116	29.6500	11.1	116.3
	2019/4/3 9:54	122.0431	29.6371	11.1	114.9
TS_5	2019/4/3 3:14	122.0323	29.6436	8.7	116.6
	2019/4/3 3:20	122.0495	29.6361	8.9	118.5
	2019/4/3 3:28	122.0685	29.6255	9.2	123.4
TS_6	2019/5/3 12:19	122.0114	29.6502	12.7	117.6
	2019/5/3 12:31	122.0563	29.6319	12.8	114.7
	2019/5/3 12:34	122.0681	29.6260	12.8	119.8

Table 4
Initial State of multi-ship encounter situation.

	Ship	Longitude/°	Latitude/°	Speed/kn	Course/°
Group A	OS	122.1103	29.5581	13.0	334.9
	TS_{11}	122.0439	29.6375	9.80	122.6
	TS_{22}	122.0709	29.6313	6.40	154.9
Group B	OS	122.1103	29.5581	13.0	334.9
	TS_{11}	122.0439	29.6375	9.80	122.6
	TS_{22}	122.0709	29.6313	6.40	154.9
	TS_{33}	122.0431	29.6371	11.1	114.9

encounter. The key points and corresponding position serial numbers are marked with the time interval of 200s, which indicates the time spot when the risk analysis and relative distances were analyzed. The serial numbers in the figure represent the positions at different times, and the same serial number represents the same time.

The risk value represents the probability that the collision cannot be avoided. When the risk value of Group A_1 was 0 at the initial moment, it means that the ship can take any actions according to the rules to pass safely from each other. When the risk value of Group B_1 was 0.17 at the initial moment, it means that there is 17% probability that the collision cannot be avoided from the perspective of the maneuvering space of the OS. According to the trajectories of the ships in Group A_1, A_2, and A_3, the target ships sail along the Xiangshan fairway, then turn south to the Western recommended route. TS_1 and OS_1 formed a head-on situation at positions ①, ②, and ③, and there was no encounter between the two ships at positions ④, ⑤, and ⑥. The minimum relative distance between the TS_1 and OS_1 was 999m at 904s. Through the relative distance analysis, the target ship in Group A_1 will not induce collision risk between the two ships, which is consistent with the results obtained by the
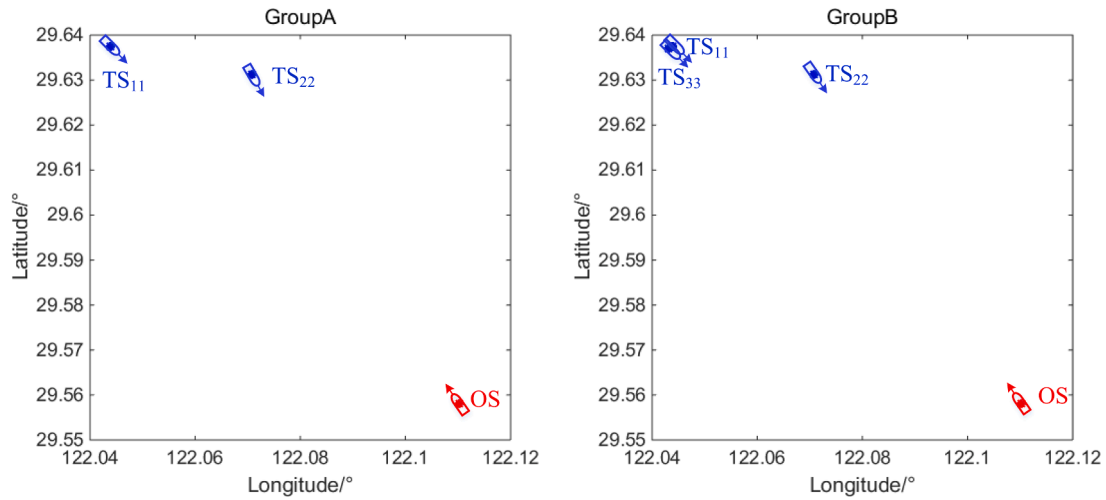
Fig. 13. The planar layout of ships for the multi-ship encounter situations.

MMSI	Time	Longitude/°	Latitude/°	Speed/kn	Course/°
TS_{11}	2019/1/3 10:19	122.0375	29.6421	9.7	125.8
	2019/1/3 10:21	122.0417	29.6389	9.8	129.1
	2019/1/3 10:22	122.0439	29.6375	9.8	122.6
TS_{22}	2019/2/3 21:05	122.0596	29.6539	6.1	153.9
	2019/2/3 21:13	122.0665	29.6411	6.3	155.6
	2019/2/3 21:19	122.0709	29.6313	6.4	154.9
TS_{33}	2019/4/3 9:38	121.9894	29.6604	11.1	118.5
	2019/4/3 9:45	122.0116	29.6500	11.1	116.3
	2019/4/3 9:54	122.0431	29.6371	11.1	114.9

Improved R-TCR value. Therefore, the risk results of Group A_1 calculated by the proposed model are in line with reality.

TS_3 and OS_3 formed crossing situations at initial positions ①, ②, and ③. It changed from crossing situation to overtaking situation at positions ④. At positions ⑤ and ⑥, the OS overtook the TS. At 1083s, the minimum relative distance between the two ships was 484m. Through the relative distance analysis, the target ship will enter the OS's domain, and there was a collision risk between the two ships. The distance between the two ships will be much closer thus the collision risk between

ships will be higher and higher. Combined with the analysis of the Improved R-TCR value, the risk results of Group A_2 calculated by the model are also in line with reality.

TS_5 and OS_5 formed overtaking situations at positions ① and ②, but there was no encounter between the two ships at positions ③, ④, ⑤, and ⑥. At 698s, the minimum actual distance between the two ships was 1397m. Through the relative distance analysis, the target ship in Group A_3 will never enter the OS's domain, and there was no collision risk between the two ships. Therefore, the risk results of Group A_3 calculated by the model are also in line with reality.

The actual situation of Group B_1, B_2, and B_3 are different from that of Group A_1, A_2, and A_3. The target ships in Group B_1, B_2, and B_3 sailed along the Xiangshan fairway without the change of route. The relative distances between Group B_1, B_2, and B_3 decreased first and then increased. For Group B_1, OS_2 and TS_2 were in a head-on encounter situation. the distance between two ships between positions ⑤ and ⑥ was the nearest. The minimum distance was about 149m. For Group B_2, OS_4 and TS_4 were always in a crossing encounter situation. Similarly, between positions ⑤ and ⑥, the distance between the two ships was the smallest, which was about 75 m. For Group B_3, the two ships were in the overtaking situation, and OS_6 was the overtaking ship. When it was near position ⑥, the actual minimum distance between the two Group B_3 was
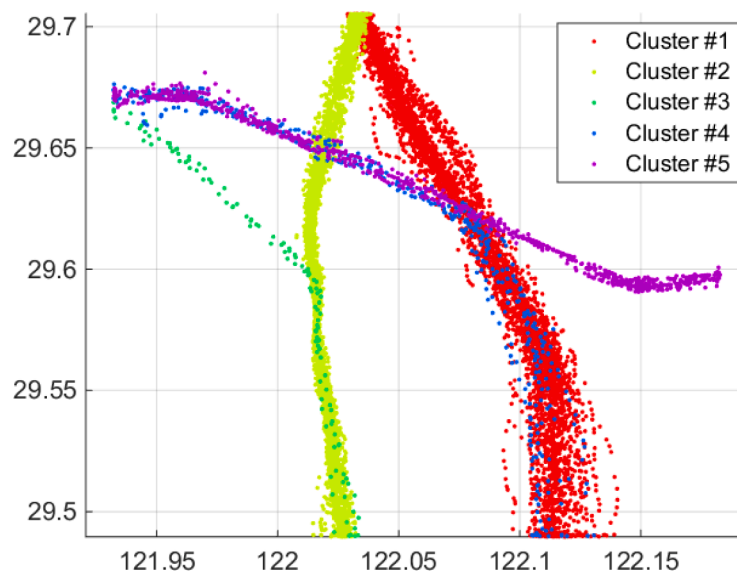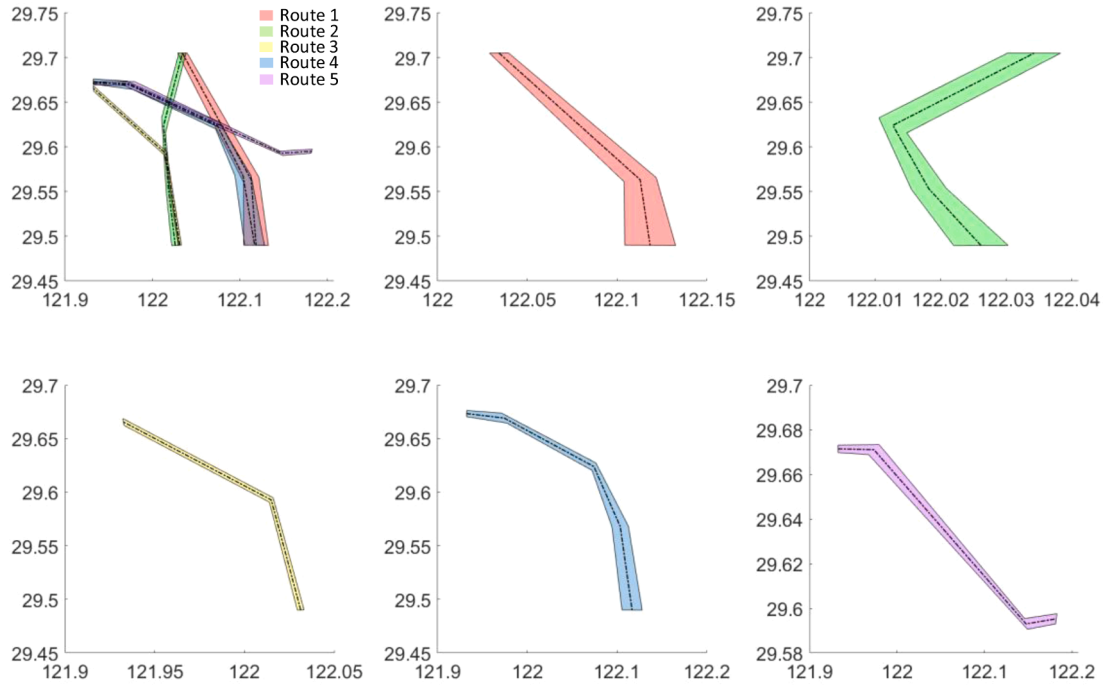

Fig. 14. Trajectory clustering results.

Fig. 15. Route identification results.

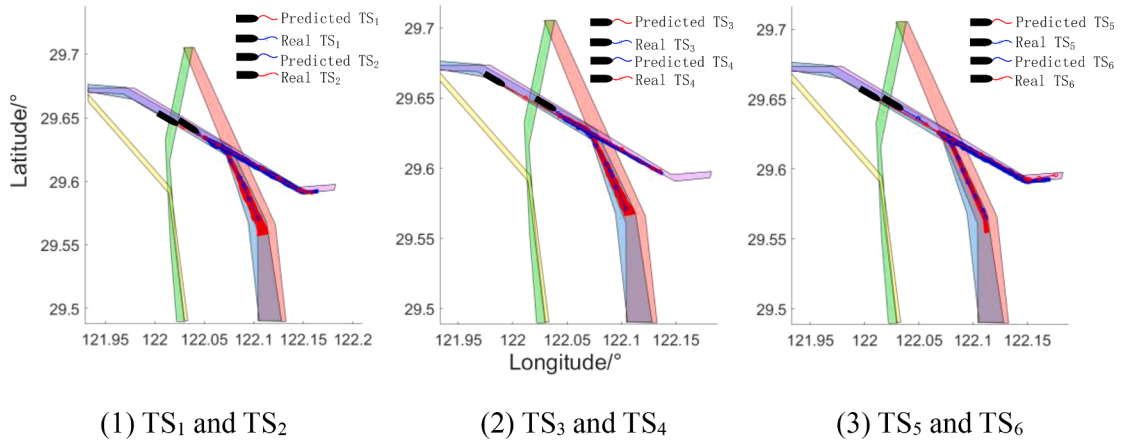(1) TS$_1$ and TS$_2$ (2) TS$_3$ and TS$_4$ (3) TS$_5$ and TS$_6$

Fig. 16. Comparison between predicted trajectory and real trajectory (two ships).

about 549m. Through the relative distance analysis, target ships entered the OS's domain, and Group B_1, B_2, and B_3 formed the risk of collision during the encounter process. Moreover, from the analysis of the distance between the two ships, the distance between the two ships became smaller with the increment of time, and there was always a collision risk between the two ships. The safe available action space between the ships becomes smaller and smaller, so the collision risk between the two ships becomes larger and larger. Combined with the analysis of the Improved R-TCR value, the risk was detected in Group B_1, B_2, and B_3. Combined with the analysis of collision risk, real trajectory, and relative distance, it can be seen that the risk results of each group are consistent with the actual situation.

Through comparative analysis between Group A and Group B, it can be seen that even in the same encounter situation, the calculation result of collision risk was different when CPA and tCPA were the same for each ship. Such as Group A_1 and Group B_1, both groups were in a head-on encounter situation. Group A_2 and Group B_2, both of which were in overtaking encounter situations. Group A_3 and B_3 were crossing encounter situations. No collision risk was detected in Group A_1, A_3. The

collision risk value of Group A_2, B_1, B_2, and B_3 always increased with the increase in time. The growth rate was low in the initial stage, but it gradually accelerated in the later stage. Therefore, ships should take avoidance action as soon as possible to solve the conflict.

4.3.2. Results of multi-ship encounter situation

The Improved R-TCR value, ship trajectories, and relative distance of multi-ship encounter situations (Group A) are shown in Fig. 20. Key points and corresponding position serial numbers are marked every 200s.

As shown in Fig. 20, the Improved R-TCR value of the ship was about 0.12 at position ①, which means that the probability that the collision cannot be avoided was 12%. At about 630s, the collision risk value was 1, which means that the collision cannot be avoided only by the effective avoidance action of OS. Please be noted that in this paper the concept of collision referred specifically to the violation of ship domain, instead of the collision accident. The value 1 of collision risk here indicates that the own ship's domain was 100% violated by target ships and the own ship was in an extremely dangerous encounter situation, which was highly
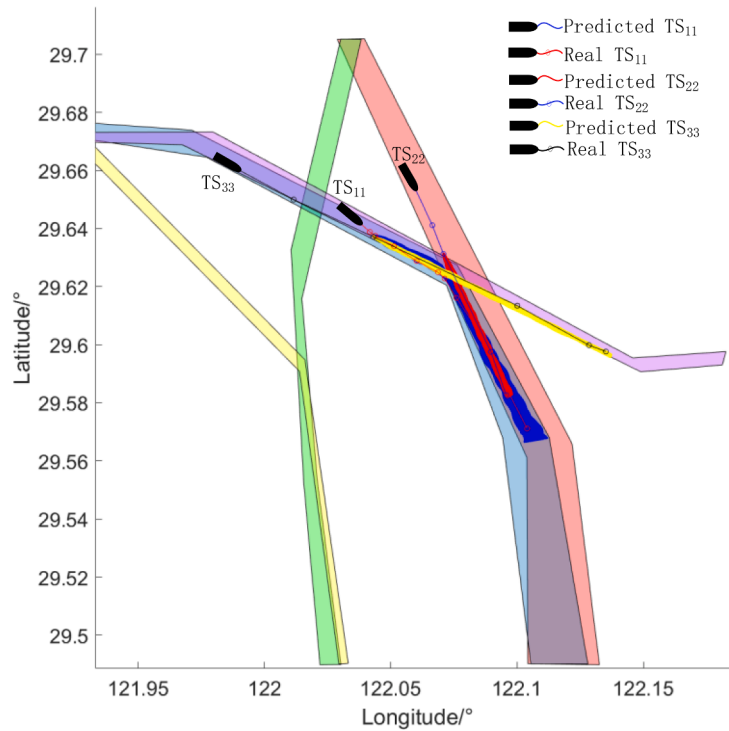
Fig. 17. Comparison between predicted trajectory and real trajectory (multiple ships).

likely to cause the accident. At positions ①, ②, ③, and ④, the OS and TS_{11} formed a crossing encounter situation; At position ⑤, the two ships formed head-on encounter situations; OS and TS_{22} were always in the head-on encounter situation. When the OS and TS_{11} are at 955s, the minimum relative distance between the two ships was 127m. When the OS and TS_{22} are at 885s, the minimum relative distance between the two ships was 43 m.

According to the analysis of the real trajectory and relative distance of OS, TS_{11}, and TS_{22}, there is a collision risk between ships. Combined with the Improved R-TCR value, the Improved R-TCR value became larger with the increment of time, which is consistent with the actual situation.

Fig. 21 shows the Improved R-TCR value, ship trajectories, and relative distance of a multi-ship encounter situation (Group B). The Improved R-TCR value was about 0.32 at position ①, which means that the probability that the ship cannot avoid collision is 32%. At 450 s, the collision risk value was 1, which means that the collision situation cannot be avoided only by the effective avoidance action of the OS and the OS was in a high-risk situation. The encounter relationship between OS and TS_{11} and TS_{22} was the same as that of Group A. As for OS and TS_{33} there was no encounter situation formed. The minimum distance between OS and TS_{33} is 1307m at 926s. Although there is no collision risk between OS and TS_{33}, it affected the maneuvering space of OS. Compared with Group A, the Improved R-TCR value of Group B was higher at the same time. The risk value of Group B reached 1 earlier than Group A, which means that the encounter of group B develops faster than that of group A with regards to the collision risk.

5. Discussion

The Improved R-TCR model is based on the original R-TCR model and considers the motion uncertainty of the target ship. Through the target ship trajectory prediction, the motion intention of the target ship can be identified, and the collision risk between ships can be calculated in combination with the ship maneuverability, COLREGs, and good seamanship.

5.1. Comparison with the CRI method

To further analyze the advantages of the proposed method, here we have compared its performance with the classic CPA-based collision risk measurement. The traditional CRI combines CPA and tCPA by the weighted method [56], as shown in Eq. (19). In this part, we mainly compare Improved R-TCR with the traditional CRI method. The parameters of the CRI method are set as follows: $\alpha_1 = 1$ and $\alpha_2 = 1$. According to the initial settings in Table 2, the values of Improved R-TCR and CRI in different encounter situations are shown in Fig. 22.

$$\text{CRI}^{(t)} = \alpha_1 \times \left(\frac{Max(TCPA^{(t)}) - TCPA^{(t)}}{Max(TCPA^{(t)}) - Min(TCPA^{(t)})} \right)^2 + \alpha_2 \times \left(DCPA^{(t)} \right)^2 \quad (19)$$

Where: $DCPA^{(t)}$ is the distance at the closest point of approach at t time; $TCPA^{(t)}$ is the time to the closest point of approach at t time.

In general, for the different encounter situations with the same initial CPA and tCPA, their risk values calculated by the CRI model are also the same. The initial CPA of Group A_1, Group B_1, Group A_2, and Group B_2 is 0nm and tCPA is 900s. The CRI value and change trend of these four groups are the same. The initial CPA of Group A_3 and Group B_3 is also 0nm, but the tCPA is 1200s. The CRI value and change trend of these two groups are exactly the same. However, according to the actual trajectory and relative distance in Figs. 18 and 19, there was no collision risk for Group A_1 and Group A_3. The collision risk value provided by the CRI method is inconsistent with the actual situation. The reason for such a result is that the CRI-based approach has assumed that the motion trend of the target ship remains constant and ignored the potential changes. The Improved R-TCR method, with its advantages in estimating the potential motion of target ships, can effectively identify such scenarios and provide the correct analysis of the collision risk.

For Group B_1, B_2, and B_3, the collision risk value estimated by the Improved R-TCR model is higher than the traditional CRI method, and the collision risk value reaches 1 earlier. According to the risk results of the CRI method, the highest risk value of Group B_1 and Group B_2 arrived at 900 s, and the highest risk value of Group B_3 arrived at the 1200 s. According to the calculation results of Improved R-TCR, the highest risk
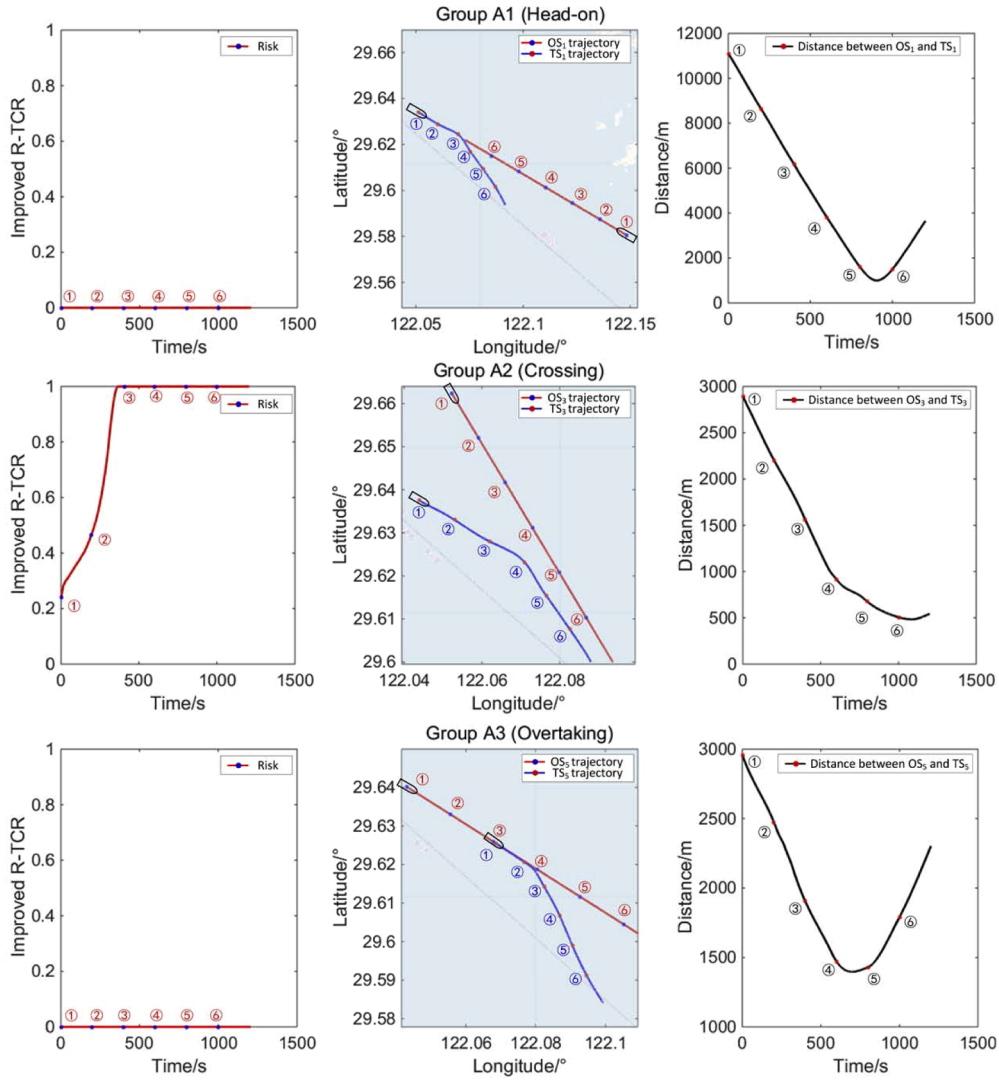
Fig. 18. Results of improved R-TCR (Group A_1, A_2, A_3).

value was reached at 405 s, 420 s, and 210 s for Group B_1, B_2, and B_3, respectively.

To sum up, compared with the CRI method, Improved R-TCR can provide an early warning with consideration of the potential motion trend of the target ships and can provide more reliable and timely risk analysis results to the decision-makers.

5.2. Comparison with the VCRO method

Section 5.2 compares the Improved R-TCR with the traditional CRI model. To further verify the effectiveness and advantage of the Improved R-TCR model, another comparison between the proposed model and the VCRO method [13] is elaborated in this section.

The VCRO method comprehensively considers the distance between the two ships, the relative speed of the ships, and the difference between the headings of the ships, and gives the risk degree between ships in combination with expert experience. Improved R-TCR value in the range of [0,1], and the VCRO value range is larger. To make the data comparable, normalize the VCRO value, and take the absolute value as the final risk value. According to the initial settings in Table 2, the Improved R-TCR and VCRO values under different encounter conditions are shown in Fig. 23.

The VCRO value is the highest when it meets the closest point of approach. If the two ships get closer, before reaching the closest point of

approach between the two ships, the VCRO value will continue to increase. After passing the closest point of approach between the two ships, the VCRO value between the two ships will decrease. However, for the Improved R-TCR, this is not necessarily. The key to Improved R-TCR value is whether the target ship will invade the ship's domain and the ship's maneuvering space during the ship's encounter. As shown in Group A_1, at 0–400 s, the risk value calculated by the Improved R-TCR model is almost consistent with that calculated by the VCRO model. After 400 s, VCRO value began to increase rapidly; Near 900 s, the VCRO value reached the peak and then began to decline. However, in this encounter process, the target ship has never entered the OS's domain. Therefore, the risk value calculated by Improved R-TCR is always 0. This means that the own ship does not need to take any avoidance action, but can also ensure the navigation safety of ships. In Group A_2, compared with Improved R-TCR, the VCRO value is unstable and fluctuates greatly. However, when using these two models, the changing trend of risk is roughly the same. The situation in Group A_3 was similar to that in Group A_1.

In Groups B_1, B_2, and B_3, the value at risk calculated by the Improved R-TCR model and VCRO model increased with time. However, the increased Improved R-TCR value will not decrease when it reaches 1, but the VCRO value will decrease when it reaches the highest value. In Groups B_1 and B_2, the growth rate of risk between ships is increasing. However, the VCRO value between the two ships increased slowly in
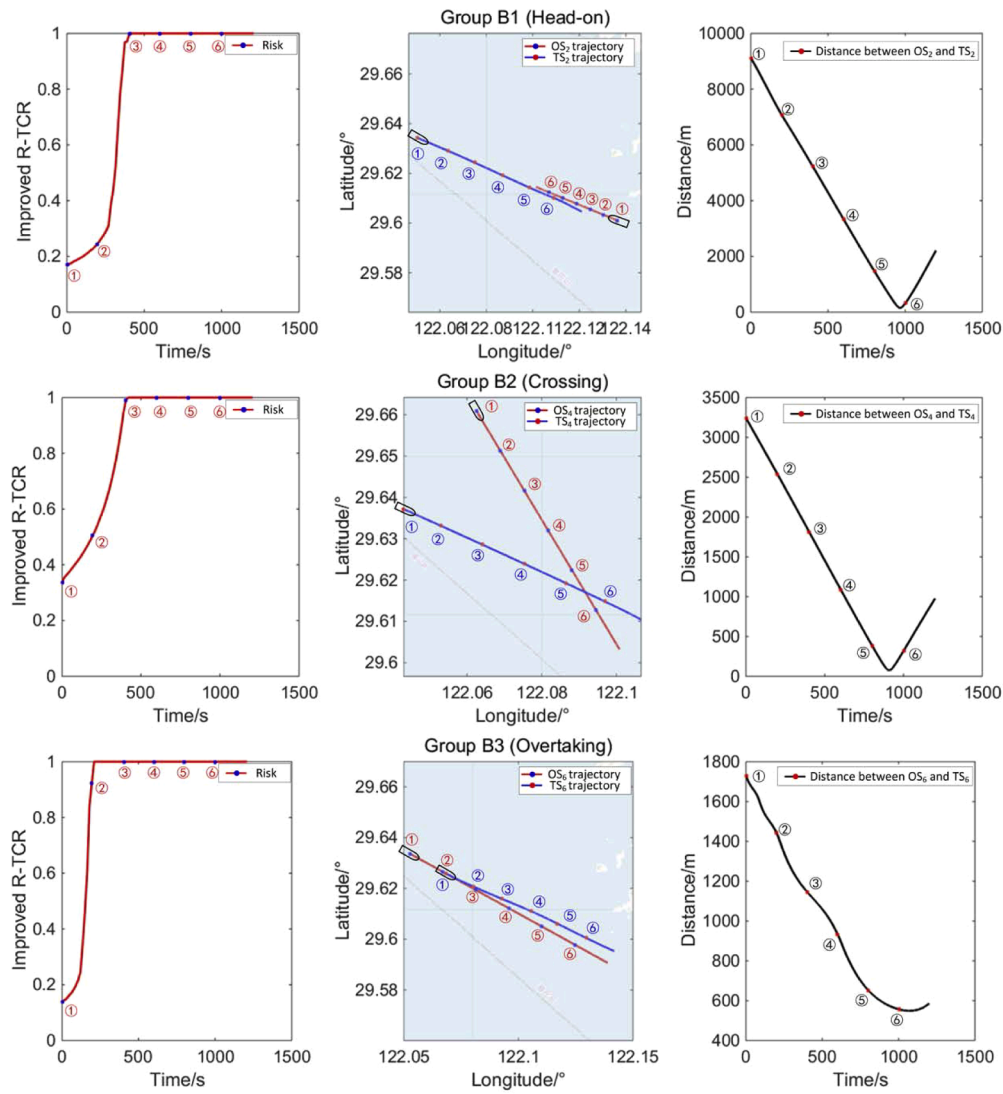
Fig. 19. Results of improved R-TCR (Group B_1, B_2, B_3).
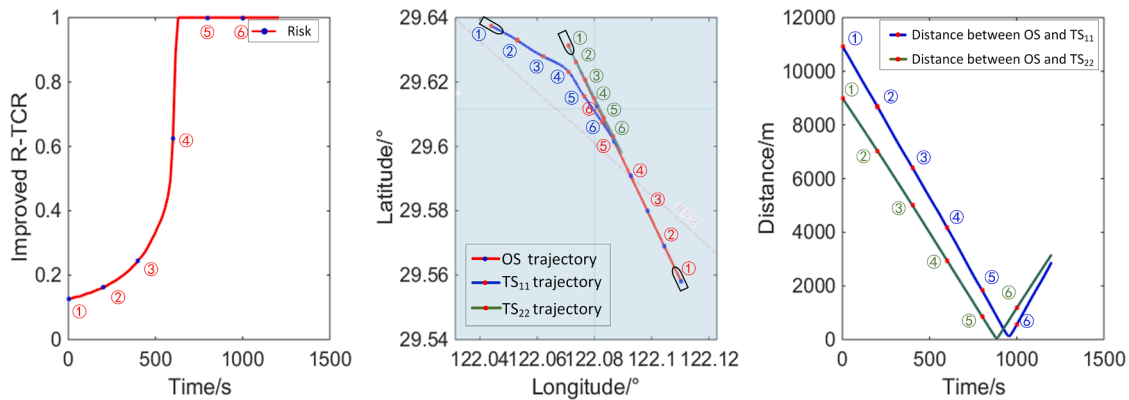

Fig. 20. Results of improved R-TCR (Group A).

Group B_3. Especially at 1000 s, the distance between the two ships is very close, and the actual risk value will be very large.

In general, the VCRO model can be used to estimate the collision risk between ships, and the value is consistent with the Improved R-TCR value at some times. However, without considering the potential motions of the target ships, similar to the conventional CRI model, the VCRO method also provided incorrect risk estimations for some encounter situations, e.g., Groups A1 and A3. Such an issue is well solved in the Improved R-TCR model. Besides, the risk analysis results of the VCRO method fluctuate significantly during the encounter process,
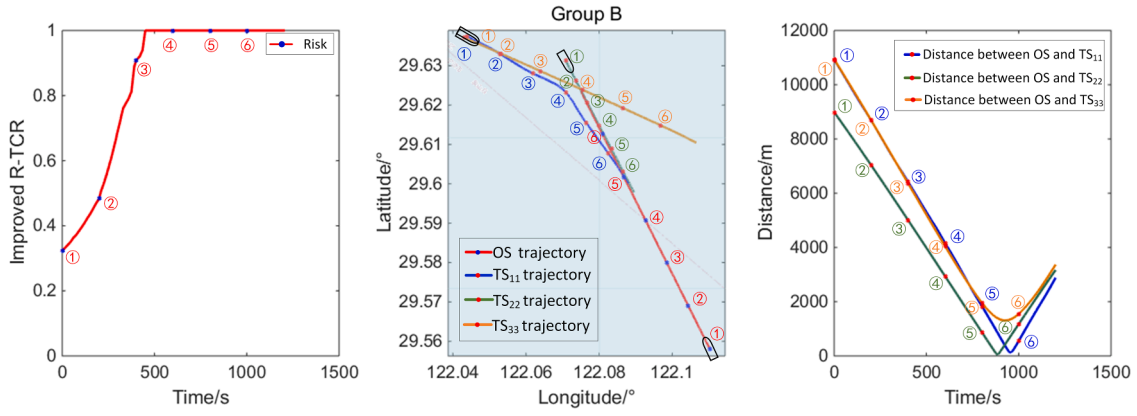
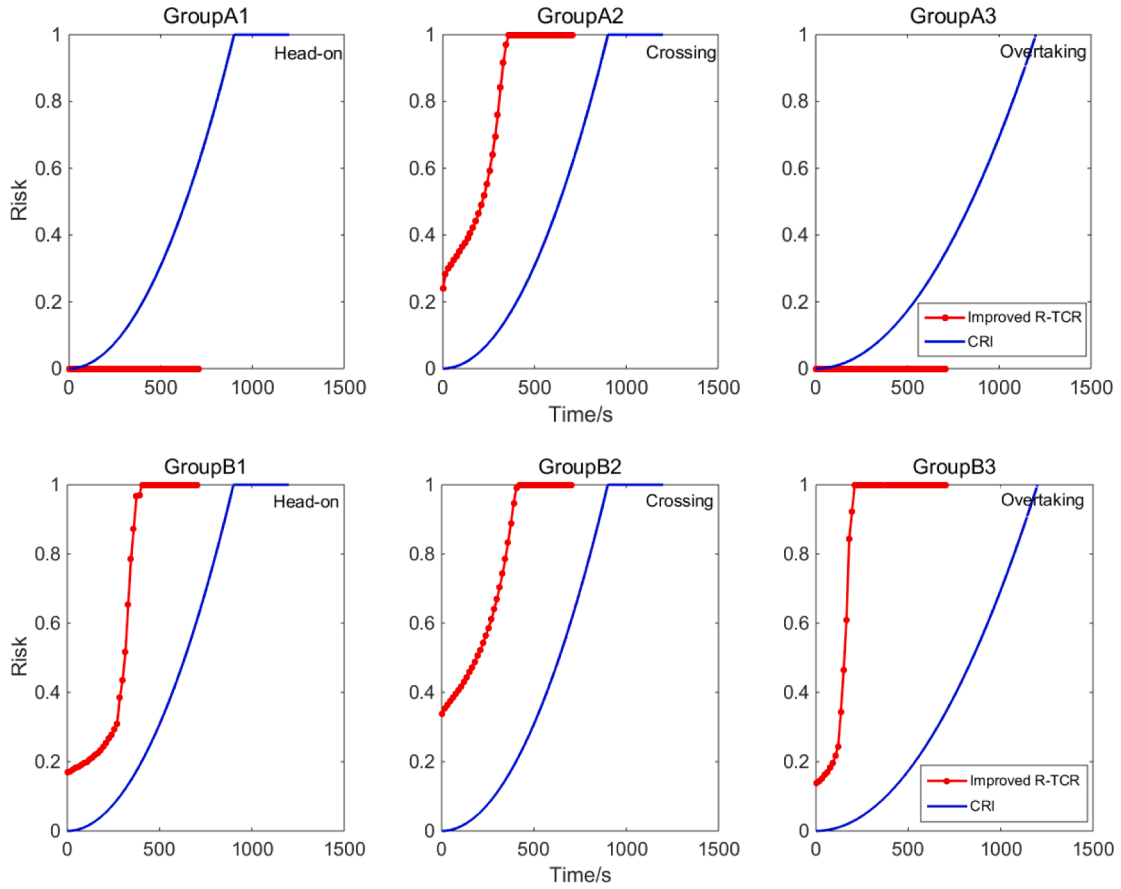**Fig. 21.** Results of improved R-TCR (Group B).

Fig. 22. . Results of improved R-TCR and CRI.

which is due to the fact that it utilizes the parameters reflecting the immediate motion of the ships. Such results could confuse the decision-makers to some extent as it may produce an inconsistent analysis of the encounter situation. Meanwhile, the Improved R-TCR could solve such an issue with relatively stable performance.

5.3. Comparison with the original R-TCR method

To further analyze the advantages of the Improved R-TCR model, it will be compared with the original R-TCR model proposed by the authors in [6]. The difference between the Improved R-TCR model and the R-TCR model lies in the consideration of avoidance action and target ship motion uncertainty. In this paper, a control experimental group will

be added, that is, the R-TCR$_1$ model will be used. Refer to Table 6 for the differences between those models. By comparing the R-TCR model with the R-TCR$_1$ model, we can analyze the impact of variable speed action on the risk model. By comparing the R-TCR$_1$ model with the Improved R-TCR model, the impact of target ship uncertainty on the risk model can be analyzed.

The risk values of each group are calculated by using the R-TCR model, R-TCR$_1$ model, and Improved R-TCR model, as shown in Fig. 24.

The green line represents R-TCR, the blue line is R-TCR$_1$, and the red line refers to Improved R-TCR. By comparing R-TCR and R-TCR$_1$, it can be seen that the impact of speed variables on risk is different in different encounter scenarios. For example, in Group B$_1$, R-TCR$_1$ value is higher than R-TCR value, which means that the risk value will be higher after
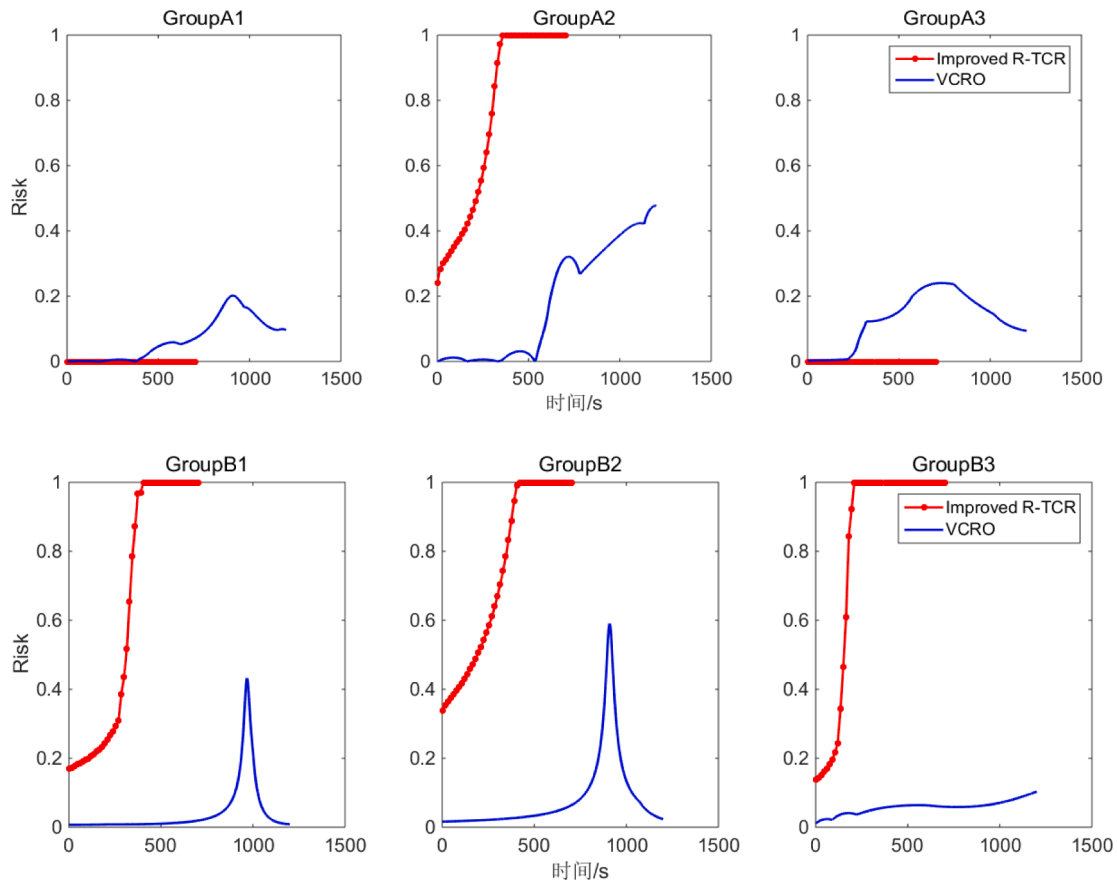
Fig. 23. Results of improved R-TCR and VCRO.

Table 6
Differences between the R-TCR and improve R-TCR models.

R-TCR	R-TCR$_1$	Improved R-TCR
The action only refers to the alteration of course.	The action only refers to the alteration of course and speed.	The action only refers to the alteration of course and speed.
Target ships keep course and speed	Target ships keep course and speed	Target ship motion uncertainty

increasing the speed alteration actions. This also shows that the speed alternation cannot effectively solve the collision in the head-on encounter situation. Speed reduction will lead to a poor steering effect and make the ship course alteration actions avoidance effect worse. As can be seen from Group A$_2$ and Group B$_2$, R-TCR$_1$ is lower than R-TCR. Thus, in the crossing encounter situation, speed alteration action has a certain collision avoidance effect. If the ship does not advance at full speed, speed alteration can solve the collision, but course alteration to avoid collision is better.

When comparing Improved R-TCR with R-TCR$_1$, R-TCR$_1$ increases over time, but according to the analysis of the real trajectory of the two ships in Section 4.3, there is no collision risk in Group A$_1$, Group A$_3$. Therefore, R-TCR$_1$ is not consistent with the actual situation. When both the R-TCR model and R-TCR$_1$ model are used to detect the collision risk, a false alarm is easy to occur. Therefore, considering target ship uncertainty, Improved R-TCR model can improve the reliability and accuracy of risk collision detection.

5.4. Advantages and limitations

The Improved R-TCR model overcomes the limitation that the

uncertainty of TS motion is not considered in the original R-TCR model and can only be applied to open waters. Combined with the above two points, the Improved R-TCR model is more in line with the actual situation than the original R-TCR model and can provide more reliable and prompt risk analysis results to the decision-makers.

Although the Improved R-TCR is improved compared with R-TCR, there are still the following limitations. Firstly, like the R-TCR model, the Improved R-TCR model also ignores the preference of OOW in collision avoidance. In future research, it is necessary to study the preference of OOW. In addition, the Improved R-TCR model considers the ship maneuverability, and a more accurate ship motion model is needed to further improve its accuracy. Finally, the Improved R-TCR model should consider the external environment, such as wind, wave, current, and channel boundary. However, the objective of this research is to propose a prediction-based collision risk model and verify its effectiveness and improvement in the risk analysis of ship encounters. These limitations will be further solved as further studies following this approach.

6. Conclusion

Maritime safety is of great significance for the global economy and society. In this paper, an Improved Rule-aware Time-varying Collision risk (Improved R-TCR) model for ship collision risk analysis is proposed. Within this research. The motion uncertainty of the target ship, the maneuverability of the OS, COLREG rules, and good seamanship are comprehensively integrated into the risk modeling utilizing the velocity obstacle method as the framework.

To overcome the uncertainty of the target ship movement and its influence on the collision risk modeling, the Gaussian process is used to predict the target ship trajectory, and the PVO algorithm is used to
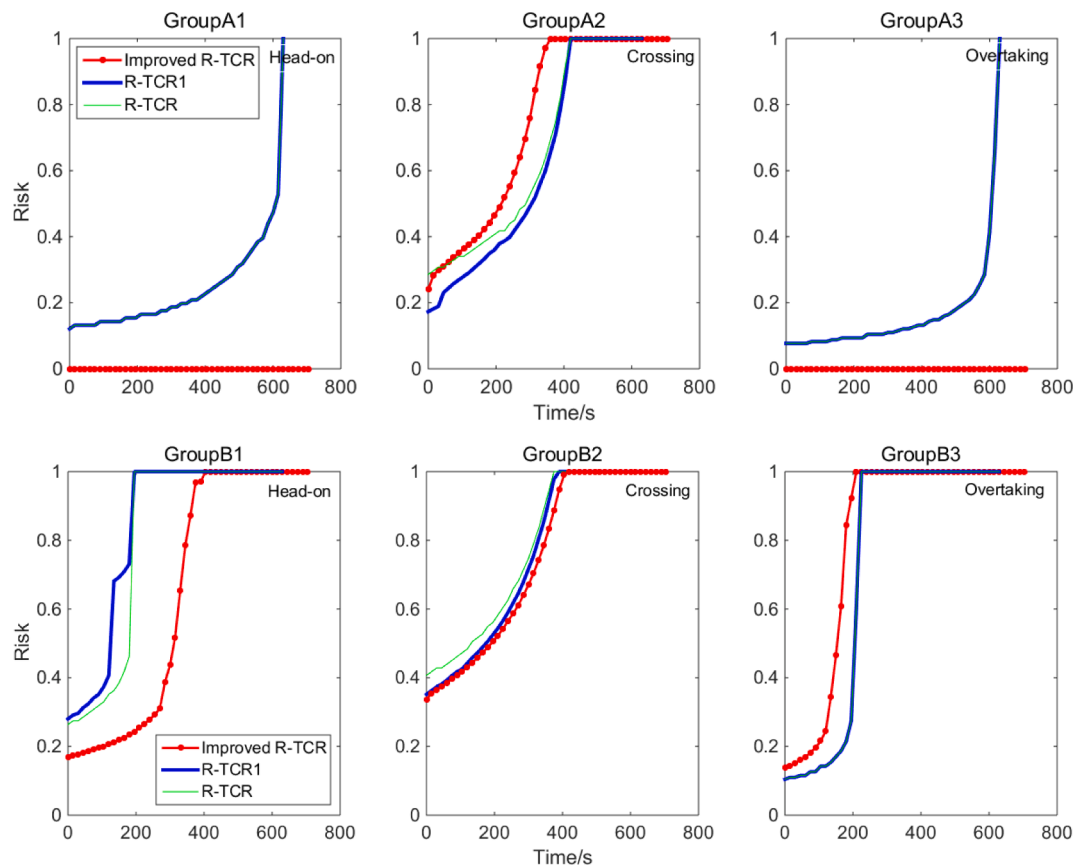
Fig. 24. Results of improved R-TCR and R-TCR.

integrate those factors into the collision risk model. The influence of the own ship maneuverability, the obligation of COLREGs regulations, and good seamanship are further integrated into the risk modeling via identifying the available actions and dangerous actions in the velocity domain of the own ship. Finally, the risk of collision between ships is quantified as the percentage of the available collision-avoidance velocities that could lead to an accident in the velocity domain of the own ship.

A series of case studies, which focus on different encounter situations are designed and executed, the results of which indicate that the model can accurately describe the risk of collision between ships under different encounter situations and different complexities, together with its characteristics of variations through the whole encounter process. To further analyze the contribution and characteristics of the proposed method, compared with the previous collision risk analysis method and the original R-TCR model, a series of comparative studies between the conventional CRI method, VCRO method, and original R-TCR model are conducted. It can be seen from the results that the work of this paper can avoid potentially inaccurate estimation of risk with its advantages on the target ship motion prediction and has more reliable results.

In conclusion, the contribution of the work compared with previous research is the improvement of the accuracy and reliability of the collision risk analysis results with the target ship motion prediction module and the comprehensive integration of factors such as COLREGs, good seamanship, etc. through a simple but concise framework of velocity obstacle method. The proposed Improved R-TCR could provide a good reference for future work on the collision risk analysis to improve the accuracy and reliability of the results.

CRediT authorship contribution statement

Mengxia Li: Conceptualization, Methodology, Investigation, Formal analysis, Writing – original draft. **Junmin Mou:** Methodology, Resources, Supervision. **Pengfei Chen:** Conceptualization, Methodology, Supervision, Writing – review & editing. **Hao Rong:** Visualization. **Linying Chen:** Methodology, Visualization. **P.H.A.J.M. van Gelder:** Supervision, Writing – review & editing.

Declaration of Competing Interest

The authors declare that they have no known competing financial interests or personal relationships that could have appeared to influence the work reported in this paper.

Acknowledgment

References

[1] Chen P, Huang Y, Mou J, van Gelder PHAJM. Ship collision candidate detection method: a velocity obstacle approach. Ocean Eng 2018;170:186–98.
[2] Li M, Mou J, Liu R, Chen P, Dong Z, He Y. Relational model of accidents and vessel traffic using AIS data and GIS: a case study of the western port of Shenzhen city. J Mar Sci Eng 2019;7(6):163.
[3] Mou JM, Tak CVD, Ligteringen H. Study on collision avoidance in busy waterways by using AIS data. Ocean Eng 2010;37(5-6):483–90.
[4] Chen P, Huang Y, Mou J, van Gelder PHAJM. Probabilistic risk analysis for ship-ship collision: state-of-the-art. Saf Sci 2019;117:108–22.
[5] Huang Y, Chen L, Chen P, Negenborn RR, van Gelder PHAJ. Ship collision avoidance methods: state-of-the-art. Saf Sci 2020;121:451–73.
[6] Li M, Mou J, He Y, Chen L, Huang Y. A Rule-aware time-varying conflict risk measure for MASS considering maritime practice. Reliab Eng Syst Saf 2021;215: 107816.

[7] Xu Q, Wang N. A survey on ship collision risk evaluation. Promet Traffic Transp 2014;26(6):475–86.

[8] Huang Y. Supporting human-machine interaction in ship collision avoidance systems. Delft University of Technology; 2020.

[9] Zhen R, Riveiro M, Jin Y. A novel analytic framework of real-time multi-vessel collision risk assessment for maritime traffic surveillance. Ocean Eng 2017;145: 492–501.

[10] Cai M, Zhang J, Zhang D, Yuan X, Soares CG. Collision risk analysis on ferry ships in Jiangsu section of the Yangtze river based on AIS data. Reliab Eng Syst Saf 2021; 215:107901.

[11] Silveira P, Teixeira A, Figueira J, Soares CG. A multicriteria outranking approach for ship collision risk assessment. Reliab Eng Syst Saf 2021;214:107789.

[12] Zhao L, Fu X. A novel index for real-time ship collision risk assessment based on velocity obstacle considering dimension data from AIS. Ocean Eng 2021;240: 109913.

[13] Zhang W, Goerlandt F, Montewka J, Kujala P. A method for detecting possible near miss ship collisions from AIS data. Ocean Eng 2015;107:60–9.

[14] Szlapczynski R, Szlapczynska J. Review of ship safety domains: models and applications. Ocean Eng 2017;145:277–89.

[15] Szlapczynski R, Szlapczynska J. A ship domain-based model of collision risk for near-miss detection and collision alert systems. Reliab Eng Syst Saf 2021;214: 107766.

[16] Fiskin R, Atik O, Kisi H, Nasibov E, Johansen TA. Fuzzy domain and meta-heuristic algorithm-based collision avoidance control for ships: experimental validation in virtual and real environment. Ocean Eng 2021;220:108502.

[17] Zheng K, Chen Y, Jiang Y, Qiao S. A SVM based ship collision risk assessment algorithm. Ocean Eng 2020;202:107062.

[18] Shah BC, Švec P, Bertaska IR, Sinisterra AJ, Klinger W, von Ellenrieder K, Dhanak M, Gupta SK. Resolution-adaptive risk-aware trajectory planning for surface vehicles operating in congested civilian traffic. Auton Robot 2016;40(7): 1139–63.

[19] Park J, Kim J. Predictive evaluation of ship collision risk using the concept of probability flow. IEEE J Ocean Eng 2017;42(4):836–45.

[20] Huang Y, van Gelder PHAJM, Wen Y. Velocity obstacle algorithms for collision prevention at sea. Ocean Eng 2018;151:308–21 (MAR.1).

[21] Wu ZL. Analysis of radar PAD information and a suggestion to reshape the PAD. J Navig 1988;41(1):130–3.

[22] Kayano J, Kumagai K. Effectiveness of the OZT taking into account with the other ships' waypoints information. In: Proceedings of the joint 17th world congress of international-fuzzy-systems-association /9th international conference on soft computing and intelligent systems (IFSA-SCIS); 2017. p. 1–5.

[23] Szlapczynski R, Krata P, Szlapczynska J. Ship domain applied to determining distances for collision avoidance manoeuvres in give-way situations. Ocean Eng 2018;165(1):43–54.

[24] Du L, Goerlandt F, Banda O, Huang Y, Kujala P. Improving stand-on ship's situational awareness by estimating the intention of the give-way ship. Ocean Eng 2020;201:107110.

[25] Johansen TA, Cristofaro A, Perez T. Ship collision avoidance using scenario-based model predictive control. IFAC PapersOnLine 2016;49(23):14–21.

[26] Candeloro M, Lekkas AM, Sørensen AJ. A Voronoi-diagram-based dynamic path-planning system for underactuated marine vessels. Control Eng Pract 2017;61: 41–54.

[27] Cho Y, Han J, Kim J. Intent inference of ship maneuvering for automatic ship collision avoidance. IFAC PapersOnLine 2018;51(29):384–8.

[28] Xie S, Garofano V, Chu X, Negenborn RR. Model predictive ship collision avoidance based on Q-learning beetle swarm antenna search and neural networks. Ocean Eng 2019;193:106609.

[29] Song L, Chen H, Xiong W, Dong Z, Mao P, Xiang Z, Hu K. Method of emergency collision avoidance for unmanned surface vehicle (USV) based on motion ability database. Pol Mar Res 2019;26(2):55–67.

[30] Blaich M, Köhler S, Reuter J, Hahn A. Probabilistic collision avoidance for vessels. IFAC PapersOnLine 2015;48(16):69–74.

[31] Huang Y, Chen L, van Gelder PHAJM. Generalized velocity obstacle algorithm for preventing ship collisions at sea. Ocean Eng 2019;173:142–56.

[32] Xin X, Liu K, Yang Z, Zhang J, Wu X. A probabilistic risk approach for the collision detection of multi-ships under spatiotemporal movement uncertainty. Reliab Eng Syst Saf 2021;215:107772.

[33] Rong H, Teixeira AP, Guedes Soares C. Ship trajectory uncertainty prediction based on a gaussian process model. Ocean Eng 2019;182:499–511.

[34] Rong H, Teixeira AP, Guedes Soares C. Maritime traffic probabilistic prediction based on ship motion pattern extraction. Reliab Eng Syst Saf 2022;217:108061.

[35] Baek KY, Bang H. ADS-B based trajectory prediction and conflict detection for air traffic management. Int J Aeronaut Sp Sci 2012;13:377–85.

[36] Yu H, Fang Z, Murray AT, Peng G. A direction-constrained space-time prism-based approach for quantifying possible multi-ship collision risks. IEEE Trans Intell Transp Syst 2021;22(1):131–41.

[37] Prandini M, Hu J. A stochastic approximation method for reachability computations, stochastic hybrid systems. Springer; 2006. p. 107–39.

[38] Chen P, Li M, Mou J. A velocity obstacle-based real-time regional ship collision risk analysis method. J Mar Sci Eng 2021;9(4).

[39] Ester M, Kriegel HP, Sander J, Xu X. A density-based algorithm for discovering clusters in large spatial databases with noise. AAAI Press; 1996.

[40] Rasmussen CE, Williams CKI. Gaussian processes for machine learning. MIT Press; 2006.

[41] Huang Y, van Gelder P. Time-varying risk measurement for ship collision prevention. Risk Anal 2020;40(1):24–42.

[42] Li M, Mou J, Chen L, Huang Y, Chen P. Comparison between the collision avoidance decision-making in theoretical research and navigation practices. Ocean Eng 2021;228:108881.

[43] Li M, Mou J, He Y, Zhang X, Xie Q, Chen P. Dynamic trajectory planning for unmanned ship under multi-object environment. J Mar Sci Technol 2021.

[44] Mou J, Li M, Hu W, Zhang X, Shuai G, Chen P, He Y. Mechanism of dynamic automatic collision avoidance and the optimal route in multi-ship encounter situations. J Mar Sci Technol 2020;26:1–18.

[45] Fujii Y, Tanaka K. Traffic capacity. J Navig 1971;24(4):543–52.

[46] Rawson A, Brito M. A critique of the use of domain analysis for spatial collision risk assessment. Ocean Eng 2021;219:108259.

[47] Fışkın R, Nasibov E, Yardimci M. A knowledge-based framework for two-dimensional (2D) asymmetrical polygonal ship domain. Ocean Eng 2020;202: 107187.

[48] Goodwin EM. A statistical study of ship domains. J Navig 1975;28(3):328–44.

[49] Davis PV, Dove MJ, Stockel CT. A computer simulation of marine traffic using domains and arenas. J Navig 1980;33(2):215–22.

[50] Du L, Banda OAV, Huang Y, Goerlandt F, Kujala P, Zhang W. An empirical ship domain based on evasive maneuver and perceived collision risk. Reliab Eng Syst Saf 2021;213:107752.

[51] Pietrzykowski Z, Magaj J. Ship domain as a safety criterion in a precautionary area of traffic separation scheme. TransNav Int J Mar Navig Saf Sea Transp 2017;11: 93–8.

[52] Zhang L, Meng Q. Probabilistic ship domain with applications to ship collision risk assessment. Ocean Eng 2019;186:106130.

[53] Yardımcı MO, Fışkın R, Nasibov E. A fuzzy rule-based approach to determine an asymmetrical polygonal ship domain. In: Proceedings of the innovations in intelligent systems and applications conference (ASYU); 2019.

[54] Wang Y, Chin H-C. An empirically-calibrated ship domain as a safety criterion for navigation in confined waters. J Navig 2016;69(2):257–76.

[55] He Y, Jin Y, Huang L, Xiong Y, Chen P, Mou J. Quantitative analysis of COLREG rules and seamanship for autonomous collision avoidance at open sea. Ocean Eng 2017;140:281–91.

[56] Kearon J. Computer programs for collision avoidance and track keeping, mathematical aspects of marine traffic. London, UK: Academic Press INC. LTD.; 1979.

[57] Rong H., Teixeira A.P., Guedes Soares C. Collision probability assessment based on uncertainty prediction of ship trajectories. 2019. p. 283-290.